การสังเคราะห์อนุภาคสังกะสีออกไซด์ขนาดนาโนด้วยปฏิกิริยาในวัฏภาคก๊าซ
เพื่อใช้สำหรับแผ่นพอลิเมอร์เรืองแสง

นางสาวธรชญาน์ สาธิตพิฐกุล

GAS - PHASE SYNTHESIS OF ZINC OXIDE NANOPARTICLES

FOR PHOTOLUMINESCENT POLYMERIC FILM APPLICATION

Ms. Thornchaya Satitpitakun

A Thesis Submitted in Partial Fulfillment of the Requirements
for the Degree of Master of Engineering Program in Chemical Engineering
Department of Chemical Engineering
Faculty of Engineering
Chulalongkorn University
Academic year 2008

Thesis Title   GAS - PHASE SYNTHESIS OF ZINC OXIDE
NANOPARTICLES FOR PHOTOLUMINESCENT
POLYMERIC FILM APPLICATION

By   Ms. Thornchaya Satitpitakun

Field of study   Chemical Engineering

Advisor   Associate Professor Tawatchai Charinpanitkul, D.Eng.
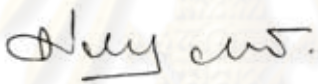
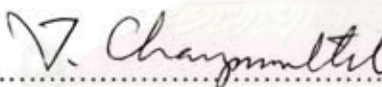Co-Advisor   Assistant Professor Anongnat Somwangthanaroj, Ph.D

Accepted by the Faculty of Engineering, Chulalongkorn University in Partial
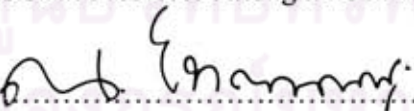Fulfillment of the Requirements for the Master's Degree

.... Dean of the Faculty of Engineering

(Associate Professor Boonsom Lerdhirunwong, Dr.Ing)
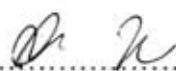
THESIS COMMITTEE

.... Chairman

(Associate Professor Prasert Pavasant, Ph.D.)

.... Advisor

(Associate Professor Tawatchai Charinpanitkul, D.Eng.)

.... Co-Advisor

(Assistant Professor Anongnat Somwangthanaroj, Ph.D)

.... Examiner

(Assistant Professor Nattaporn Tonanon D.Eng)

.... External Examiner

(Assistant Professor Akkarat Wongkaew, Ph.D.)

ธรชญาน์ สาธิตพิฐกุล : การสังเคราะห์อนุภาคสังกะสีออกไซด์ขนาดนาโนด้วยปฏิกิริยา ในวัฏภาคก๊าซเพื่อใช้สำหรับแผ่นพอลิเมอร์เรืองแสง(GAS - PHASE SYNTHESIS OF ZINC OXIDE NANOPARTICLES FOR PHOTOLUMINES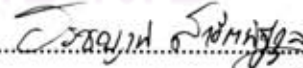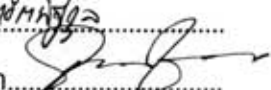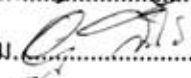CENT POLYMERIC FILM APPLICATION), อ. ที่ปรึกษาวิทยานิพนธ์หลัก: รศ.ดร. ธวัชชัย ชรินพาณิชกุล, อ. ที่ปรึกษาวิทยานิพนธ์ร่วม: ผศ. ดร.อนงค์นาฏ สมหวังธนโรจน์, 80 หน้า.

ในงานวิจัยนี้ประสบความสำเร็จในการสังเคราะห์อนุภาคสังกะสีออกไซด์ขนาดนาโนเมตรซึ่งมีสัณฐาน วิทยาที่แตกต่างกันด้วยวิธีการทำปฏิกิริยาในวัฏภาคก๊าซ โดยศึกษาอิทธิพลของอัตราการไหลของออกซิเจน อัตรา การไหลของไนโตรเจน รวมทั้งตำแหน่งในการเก็บอนุภาคและนำมาศึกษาการกระจายตัวของขนาดและสัณฐาน วิทยาของอนุภาค จากสัณฐานวิทยาของอนุภาคสังกะสีออกไซด์ที่สังเคราะห์ได้พบว่าการเพิ่มขึ้นของอัตราการ ไหลของออกซิเจนมีผลต่อการเปลี่ยนสัณฐานวิทยาของสังกะสีออกไซด์ที่สะสมบนท่อปฏิกรณ์มีรูปร่างจากแบบ ทรงสี่ก้านเป็นแบบแผ่น การเก็บอนุภาคโดยการใช้แผ่นกรองทำให้เกิดอนุภาคสังกะสีออกไซด์ที่มีรูปร่างเกือบ เป็นทรงกลม การเพิ่มขึ้นของอัตราการไหลของออกซิเจนในระบบที่ถูกปรับปรุงวิธีการเก็บอนุภาคสามารถทำให้ เกิดขาขนาดสั้นของอนุภาคสังกะสีออกไซด์ และเมื่ออัตราการไหลของไนโตรเจนเพิ่มขึ้นขนาดของอนุภาค สังกะสีออกไซด์ที่สังเคราะห์ได้จะมีขนาดเล็ก

นอกจากนั้นงานวิจัยนี้ได้ทำการศึกษาคุณสมบัติการเปล่งแสงของฟิล์มประกอบแต่งระหว่างพอลิเมทิล เมทาคริเลต หรือ พีเอ็มเอ็มเอ และสังกะสีออกไซด์ซึ่งถูกสังเคราะห์ด้วยวิธีการหลอมผสมด้วยเครื่องบดผสมแบบ สองลูกกลิ้ง อนุภาคสังกะสีออกไซด์สามชนิดซึ่งมีขนาด และความเข้มข้นที่แตกต่างกันถูกใช้เพื่อศึกษาสภาวะที่ เหมาะสมสำหรับการเตรียมวัสดุประกอบแต่งซึ่งมีคุณสมบัติทางแสง และคุณสมบัติทางกลที่ดีขึ้น พบว่าฟิล์ม วัสดุประกอบแต่งที่เตรียมจากอนุภาคสังกะสีออกไซด์ที่ถูกสังเคราะห์ขึ้นแสดงคุณสมบัติการเปล่งแสงที่ดีขึ้นเมื่อ เปรียบเทียบกับอนุภาคสังกะสีออกไซด์ทางการค้า สิ่งที่น่าสนใจอีกอย่างคือ อนุภาคสังกะสีออกไซด์ที่มีขนาดนา โนเมตรมีประสิทธิภาพในการป้องกันรังสียูวีที่มากขึ้นเมื่อเปรียบเทียบกับอนุภาคสังกะสีออกไซด์ที่มีขนาด ไมโครเมตร คุณสมบัติในการการดูดซับรังสียูวี และการป้องกันรังสียูวีของฟิล์มวัสดุประกอบแต่งจะขึ้นอยู่กับ ชนิด และความเข้มข้นของอนุภาคสังกะสีออกไซด์ที่ถูกเติมเข้าไป นอกจากนี้ยังพบว่าการการผสมกันของอนุภาค สังกะสีออกไซด์ในพีเอ็มเอ็มเอไม่ส่งผลกระทบต่ออุณหภูมิการเปลี่ยนเนื้อแก้วของฟิล์มวัสดุประกอบแต่ง

| ภาควิชา	วิศวกรรมเคมี	ลายมือชื่อนิสิต	
สาขาวิชา	วิศวกรรมเคมี	ลายมือชื่อ อ.ที่ปรึกษาวิทยานิพนธ์หลัก	
ปีการศึกษา	2551	ลายมือชื่อ อ.ที่ปรึกษาวิทยานิพนธ์ร่วม	

4970350021: MAJOR CHEMICAL ENGINEERING

KEYWORDS: ZnO / GAS PHASE REACTION / PMMA / COMPOSITE/ LUMINECENCE

THORNCHAYA SATITPITAKUN: GAS - PHASE SYNTHESIS OF ZINC OXIDE NANOPARTICLES FOR PHOTOLUMINESCENT POLYMERIC FILM APPLICATION. ADVISOR ASSOC. PROF. TAWATCHAI CHARINPANITKUL, D.Eng., CO-ADVISOR: ASSIS PROF. ANONGNAT SOMWANGTHANAROJ, Ph.D., 80 pp.

ZnO nanoparticles with various morphologies were successfully synthesized by a gas phase reaction in this work. Effects of O_2 and N_2 flow rate as well as position for collecting particle on the synthesized ZnO characteristics, which are particle size distribution and morphology were investigated. An increase in O_2 flow rate resulted in morphological change of ZnO tetrapods which were deposited on the reactor wall into plate-like morphology. Particle collection using particle filter could give rise to ZnO particles with a nearly spherical shape. Meanwhile, an increase in O_2 flow rate in the system with improved collecting method could lead to short pod of ZnO particles. When N_2 flow rate was increased the size of ZnO particle was decreased.

In addition, photoluminescence of poly(methylmetacrylate) (PMMA) and ZnO composite film, which was fabricated by the melt mixing method with a two-roll mill, was studied in this work. Three types of ZnO particles with different nominal sizes and concentrations were employed to investigate the optimal conditions for preparing the composite with preferable optical and mechanical properties. It was found that the composite films prepared from originally synthesized ZnO particles could exhibit the much improved photoluminescent property when compared with commercial ZnO particles. Interestingly, ZnO nanoparticles could effectively shield UV irradiation when compared with the micrometer-size ZnO particles. The UV absorption and shielding of composite film depended on type and concentration ZnO particles added. It was also found that mixing of ZnO particles into PMMA did not affect the glass transition temperature of the composite films.
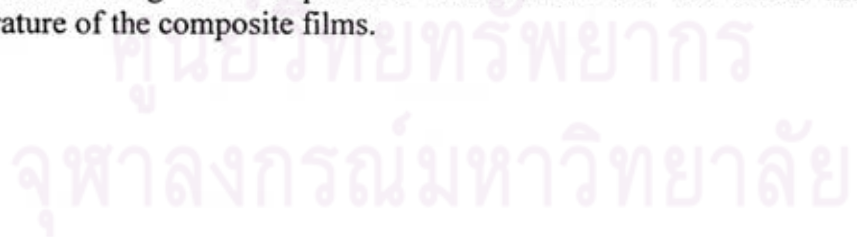
Department:.............Chemical Engineering...........Student's Signature......................

Field of Study:.......Chemical Engineering...........Advisor's Signature.....................

Academic Year:..........2008.........................Co-advisor's Signature...................

ACKNOWLEDGEMENTS

CONTENTS

LIST OF TABLES

LIST OF FIGURES

NOMENCLATURES

p_A	=	Partial pressure of component A
p_T	=	Total pressure of system
λ	=	wavelength
SEM	=	Scanning electron microscopy
XRD	=	X-Ray Diffraction
DMA	=	Dynamic Mechanical Analysis
PL	=	Photoluminescence
UV-vis	=	UV-Vis spectrophotometer
T	=	Temperature
°C	=	Degree Celsius
nm	=	nanometer
µm	=	micrometer
PMMA	=	Polymethyl methacrylate

CHAPTER I

INTRODUCTION

1.1 Background

Zinc Oxide (ZnO) is a semiconducting material with a wide bandgap of 3.3 eV and a large exciton binding energy of 60 meV [1]. Accordingly, ZnO is an important electronic and photonic material which could be used for UV light-emitters, gas sensors and acoustic wave devices. Recently, ZnO nanoparticles have attracted considerable attention due to their unique physical properties caused by the nanosized effect. Several studies have been conducted on their synthesis and structural property characterization. Several methods are used for synthesis ZnO such as sol-gel, chemical vapor deposition and gas phase reaction. Gas phase reaction method is advantage because it can operate as a continuous process. Beside products is high yield and purity. It is also used in industrial scale production which is called French Process. Moreover gas phase reaction method was simple, low cost and reduced need for apparatuses [2].

Metal or semiconductor nanoparticles dispersed in polymeric matrices have been widely studied recently. These nanocomposites exhibit interesting properties and could be widely applied to the microelectronic and optoelectronic industries. Polymethyl methacrylate (PMMA) is a promising matrix for these nanocomposites because of its good thermal stability and chemical resistance. The mechanical, electrical and optical properties of pure PMMA are further improved by including inorganic materials. Combining ZnO nanoparticles with any polymer could exhibit modified optical properties such as high intensity fluorescence and high radiation durability. ZnO/polymer composites have been produced with different polymer matrices, such as poly-vinyl pyrrolidone (PVP), poly-vinyl alcohol (PVA), [2] poly(hydroxyethyl methacrylate) [3] and polyimids [30] . So we are interested in homogeneous dispersion of ZnO in PMMA due to expected very unique optical characteristics such as high photoluminescence, high transparency, and high radiation durability which could be applied in optoelectronics, light emitting diodes, photonics and display industries in the future.

In the present work, preparation and characterization of ZnO nanoparticles via controlled synthesis of gas phase reaction was investigated. Controlling the O_2 and N_2 flow rate is the key issue in the synthesis of ZnO nanoparticles with a particular shape. The effects of size and concentration of ZnO particles on luminescence of composite, UV adsorption and dynamic mechanical properties were studied and discussed.

1.2 Objectives of research

- To synthesize ZnO nanoparticles by gas phase reaction of pure zinc particles
- To fabricate nanocomposite of ZnO nanoparticles with PMMA for preparing photoluminescent films

1.3 Scope of research

1.3.1 To conduct ZnO nanoparticles using gas phase reaction

    To Control parameters which will be taken into account are;

      a) Oxygen and nitrogen flow rate

      b) Collecting method for synthesized ZnO nanoparticles

    To Characterize morphology of synthesized ZnO by

      - X-ray diffraction (XRD)

      - Scanning Electron Microscopy (SEM)

      - Transmission Electron Microscopy (TEM)

1.3.2 To Prepare ZnO/PMMA nanocomposite

    To Control parameter taken into account are;

      a) Size of ZnO in PMMA

      b) Concentration of ZnO in PMMA

    To Characterize ZnO/PMMA composite by

    - Dynamic mechanical analysis (DMA)

    - Scanning Electron Microscopy (SEM)

    - Scanning Luminescence Spectrophotometer

    - UV-Vis spectrophotometer (UV-vis)

1.4 Procedure of the research

    1.4.1 Survey and review related literatures

    1.4.2 Synthesize ZnO by gas phase reaction

    1.4.3 Perform preliminary experiments to find out suitable conditions for preparing

ZnO/PMMA film composites

    1.4.4 Analyze and conclude the experimental results

    1.4.5 Prepare a manuscript for journal publication and thesis

1.5 Obtained Benefits

    1.5.1 Knowledge of ZnO synthesis will be obtained.

    1.5.2 Understanding the effect of filler content in polymer matrix on

photoluminescence property of film composite

CHAPTER II

FUNDAMENTAL KNOWLEDGE AND LITERATURE REVIEW

2.1 Zinc Oxide (ZnO)

Zinc oxide is a chemical compound. Its chemical symbol is ZnO. A molecule of zinc oxide consists of one zinc atom bound to one oxygen atom. It is nearly insoluble in water but soluble in acids or alkalis. It occurs as white hexagonal crystals or a white powder commonly known as zinc white as shown in Figure 2.1. The ZnO structures are hexagonal which is shown in Figure 2.2.

Fig.2.1 Zinc Oxide
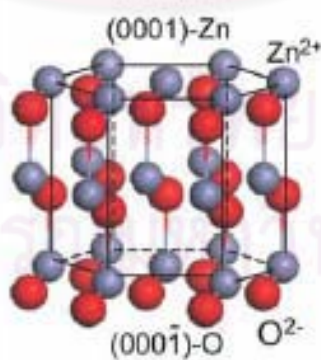
Fig 2.2 Zinc Oxide Structure

(Ref. http://www.fhi-berlin.mpg.de/th/personal/hermann/ZnO.gif)

Table 2.1 The property of zinc oxide

Properties	Value
Band Gap Energy	3.3 eV
Exciton binding Energy	60 meV
Molecular weight	81.38
Density	5.67 g/cm^3
Melting point	1975°C

2.2 Synthesis of ZnO nanostructures

Usually ZnO particles were synthesized by two methods, which are French process and American process.

2.2.1 French process

Metallic zinc is melted in a graphite crucible and vaporized above 900 °C. Zinc vapor reacts with the oxygen in the air to give ZnO, accompanied by a drop in its temperature and bright luminescence. Zinc oxide particles are transported into a cooling duct and collected in a bag house. This indirect method is commonly known as the French process (FP) which was popularized by LeClaire (France) in 1844. In a typical FP, zinc oxide normally consists of agglomerated zinc oxide particles with an average size of 0.1 micrometres to a few micrometres. By weight, most of the world's zinc oxide is manufactured via French process. Major applications involve industries related to rubber, varistors, sunscreens, paints, healthcare, and poultry nutrients. Recent developments involve acicular nanostructures (rods, wires, tripods, tetrapods, plates) synthesized using a modified French process known as catalyst-free combust-oxidized mesh (CFCOM) process. ZnO nanostructures usually have micrometre-length nanorods with nanometric diameters (below 100 nm). [19]

American process

The American process for the zinc oxide production of zinc oxide directly from oxidized ore was developed in 1851. American process zinc oxide, also is called "direct ZnO", results from the reduction by coal, and the products of partial combustion, particularly carbon monoxide, of oxidized zinciferous materials to produce zinc vapour. The zinc vapour is subsequently oxidized. In the early stages the zinc raw materials were used to be oxidized ores or roasted sulfide concentrates. Nowadays the industry mostly uses technical grade oxides obtained from refining the fine fraction of brass ashes. Other zinc raw materials that can be used are : Waelz oxides (after purification), dusts from tyre incineration, zinc carbonate and hydroxide, blowings and metalling residues, off grade zinc oxides. The zinc raw materials are mixed with coal and smelted in gas heated rotary kilns. The resulting zinc oxide is piped through a dust chamber for elimination of the coarse agglomerates and collected in bag filters for packaging. American process zinc oxides are particularly well suited for paint, ceramic and rubber industry.[20]

2.3 Application of zinc oxide

ZnO were applied in many fields such as plastics, ceramics, cosmetics and rubber.

Plastics

Zinc compounds can provide a variety of properties in the plastic field. Heat resistance and mechanical strength are imparted to acrylic composites by zinc oxide. Zinc Oxide was used to the formation and cure of epoxy resin. Addition of Zinc Oxide to epoxy resins impact to polyamines imparts higher tensile strength and water resistance. Zinc Oxide imparts fire-resistant properties to nylon fibers and moldings. Zinc Oxide is also useful in the preparation of nylon polymers and in increasing their resistance. The formation of Zinc Oxide in polyesters increases the viscosity and other improvements. ZnO reacts with unsaturated polyesters to form higher viscosity. The dye ability of polyester fibers is improved by Zinc Oxide. Zinc Oxide mixtures stabilize polyethylene against aging and ultraviolet radiation. Polyolefin's are improved in color, tensile strength, and vulcanization properties by addition of Zinc Oxide. Thermal stabilization of PVC is effected by Zinc Oxide.

Ceramics

The properties imparted by Zinc Oxide to some of the newer applications are as electronic glass, low-melting glass for metal-to-glass and devitrified glasses of low thermal expansion. Zinc Oxide imparts a unique combination of properties when used in glass. Zinc Oxide reduces the coefficient of thermal expansion, imparts high brightness and high stability against deformation under stress.

Cosmetics

The optical and biochemical properties of Zinc Oxide impart special features to a variety of cosmetic preparations for care of the hair and skin. In powders and creams it protects the skin by absorbing the ultraviolet sunburn rays; in burn ointments it aids healing.

Rubber

The rubber industry, in its development over the past one hundred years, has utilized an increasing number of the many optical, physical and chemical properties of Zinc Oxide. Zinc Oxide proved the most effective activator to speed up the rate of cure with the new accelerators. Heavy-duty pneumatic tires carry high loadings of Zinc Oxide for heat conductivity as well as support since heat-buildup is critical at their higher operating speeds compared with their solid-rubber counterparts.

2.4 Poly (methyl methacrylate) (PMMA)

Polymethyl methacrylate (PMMA), whose monomer is methyl methacrylate (MMA) is common used to produce transparent plastics. Boiling point of MMA is 105.5 °C and density is 0.936 - 0.940 g/cm^3. PMMA is a thermoplastic whose boiling point is 200°C, density 1.1 g/cm^3 and glass transition temperature 105°C. Structure of MMA and PMMA are shown in Figure 2.3. Methyl methacrylate can be converted into high molecular weight product by all the methods use for radical polymerization (bulk, emuision and suspension polymerization). PMMA has many trade names such as

Plexiglas, Perspex, Plazcryl, Acrylite, Acryplast, Lucite and Acrylic. It shows several properties, i.e. resistance to high energy radiation and chemicals, higher impact strength and good transmission. Therefore PMMA can be used for furniture makers, medical technologies, police vehicles and semiconductor research [6]
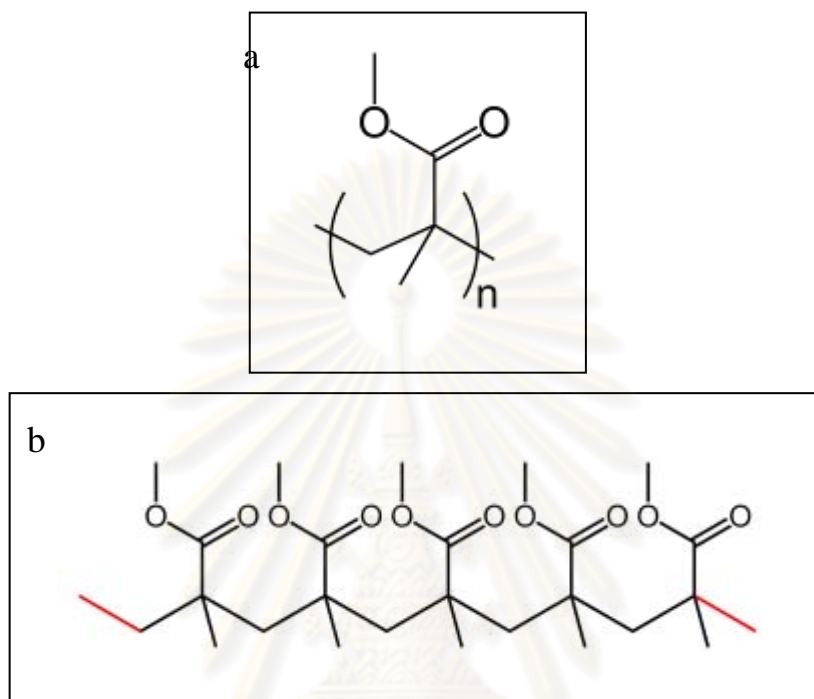
Fig 2.3 a) MMA structure and b) PMMA structure

2.5 Partial pressure

In a mixture of ideal gases, each gas has a partial pressure which is the pressure which the gas would have if it alone occupied the volume.[1] The total pressure of gas mixture is the sum of the partial pressures of each individual gas in the mixture. The partial pressure of gas dissolved in liquid is the partial pressure of that gas which would be generated in gas phase in equilibrium with the liquid at the same temperature. The partial pressure of gas is a measure of thermodynamic activity of the gas's molecules. Gases will always flow from a region of higher partial pressure to one of lower pressure; the larger this difference, the faster the flow. Gases dissolve, diffuse, and react according to their partial pressures, and not necessarily according to their concentrations in gas mixture

$$\text{Volume fraction of gas A} = \frac{p_A}{p_T}$$

Where p_A is the partial pressure of component A and $p_T = \sum p_i$ is the total pressure of the system.

The saturation vapor pressure, also called the vapor pressure, is the pressure required to maintain vapor in mass equilibrium with the condensed vapor (liquid or solid) at specified temperature. When the partial pressure of vapor equals its saturation vapor pressure, evaporation from the surface of liquid just equals condensation on that surface, and there is mass equilibrium at the surface.

The equilibrium water vapor pressure for plane surface p_s is the partial pressure p of water vapor that defines a condition of *saturation.* If, at any given temperature, the partial pressure is less than p_s, then the vapor is unsaturated, and if p is greater than p_s, the vapor is *supersaturated*. The *saturation ratio, S_R,* is the ratio of the partial pressure of vapor in a system to the saturation vapor pressure for temperature of the system.

2.6 Two-roll mill

The two-roll mill is an instrument for mixing or blending martial such as polymer and rubber. Two-roll mill is made up of corrosion resistant steel, surface hardened and polished. High temperature sealing are used for the standings. The machine comprises two drive motors installed under the roll unit. The drive motors is separated from the electrical side through roller chains on one side of the machine. Both rolls run at a stable speed and with a constant friction ratio. The motors are equipped with frequency converters which permit to adjust friction of one of the rolls, speed of both rolls, and a free adjustment of speed and friction. Temperature of two rolls can be sensed individually by a separate thermocouple system. The surface of the rolls is hard chrome plated, ground and mirror polished. The cooling of this roll is done by water cooling arrangement and water is collected in a stainless steel water collecting tank which is at the other end of roll.

2.7 Nanostructured composite [5]

Nanocomposite is a special class of materials having unique physical properties. The properties of nanocomposites can be obtained by imparting the characters of parent constituents to single material. Combining polymer and inorganic will produce an interesting materials with superior properties.

2.8 Photoluminescence [7]

Photoluminescence includes fluorescence as well as phosphorescence depending on whether the radiative transition is a spin-allowed transition between two states with equal multiplicity (singlet – singlet and, sometimes, triplet-triplet) or a spin-forbidden transition between two states with different multiplicities (triplet-singlet). The schematic energy-level diagram in Figure 2.4 shows the principal pathways by which these transitions occur. In most cases, molecules are raised from the ground state (S0) to an excited singlet state (Sn) by absorption. The facored path for deexcitation is the one which minimizes the lifetime of excited state. Almost all molecules drop quickly to the lowest levels (S1 or T1) by the nonradiative processes; therefore, the most commonly observed irradiative transitions are S1 which is S0 fluorescence and T1 which is S0 phosphorescence.
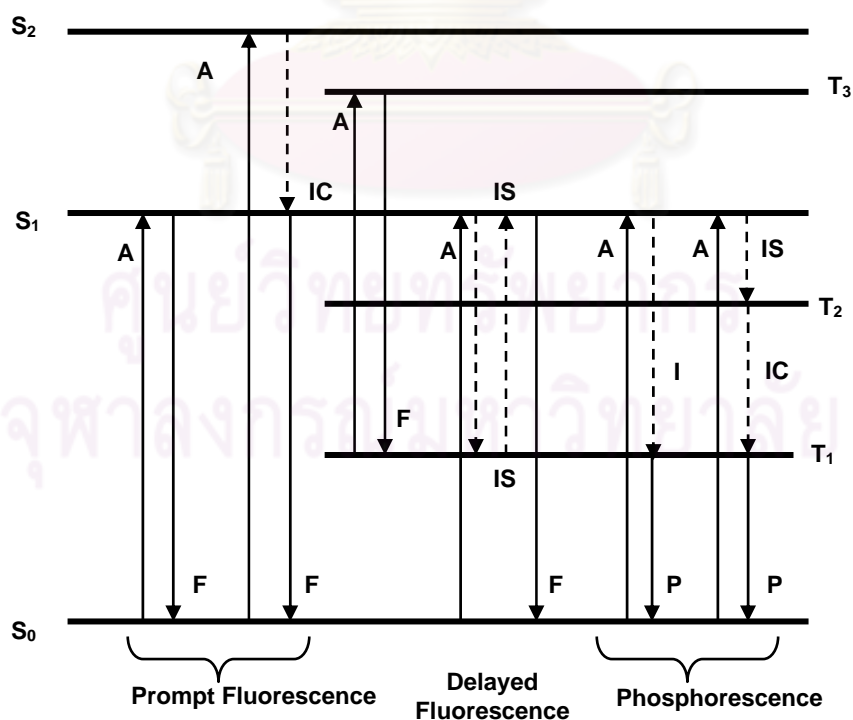
Fig 2.4 Electrons spin in molecule

➤ Principal radiative (   ) and nonradiative   (   ) transitions causing photoluminescence. S0,S1…….singlet levels; T1,T2……triplet levels. A: absorption (10^{-18} –10^{-15}s) IC: internal conversion (~10^{-12}s). IS: intersystem crossing (~10^{-9}s) F: fluorescence(10^{-10}-10^{-8}s) P: phosphorescence (10^{-3}-10s)

In general, fluorescence lifetime (0.1 – 10 ns) is much shorter than phosphorescence lifetime (1 ms to 10s), and thus fluorescence has also been difined as photoluminescence which occurs after excitation, while phosphorescence is discennibly delayed. Because the existence of delayed fluorescence with lifetime is similar to phosphorescence lifetime, this definition is not quite corrected. However, it is convenient from an operational point of view since delay fluorescence is rare, and since any emission which is delayed by less than the time constants of the detection system cannot be distinguished from prompt fluorescence with an ordinary spectrofluorometer. Likewise, phosphorescence and delayed fluorescence require similar measurement techniques; therefore, they can be considered alike from this point of view. In table 2.2, the term fluorescence is used in the sense of this operational definition as photoluminescence with lift times shorter than the time constants of the detection system.

Table 2.2 Luminescence is classified according to the mode of excitation as follows:[18]

Absorption of light	photoluminescence
High – energy particles	radio luminescence
Cathode rays, electron beams	cathode luminescence
Electric fields	electro luminescence
Thermally activated ion recombination	themo luminescence
Chemical reaction usually oxidation	chemi luminescence
Biological processes usually enzymatic	bio luminescence
Friction and static forces	tribo luminescence
Sound and ultrasound	sono luminescence

2.9 Band gap energy

Band gap, is an energy range in a solid where no electron states exist. For insulators and semiconductors, the band gap generally refers to the energy difference (in electron volts) between the top of the valence band and the bottom of the conduction band. Band gap is the amount of energy required to free an outer shell electron from its orbit about the nucleus to a free state. The wavelength of the photon is obtained from the equation relating the band gap energy to the frequency when factor in the relationship between frequency and wavelength following equation (1).

$$E = hc/wavelength. \qquad\qquad (1)$$

Where E is band gap energy(eV), h is Planck constant (6.63×10^{-34}J.s) and c is light speed (3×10^{8}m/s)

2.10 Visible light

The visible light spectrum is the section of the electromagnetic radiation spectrum that is visible to the human eye. It ranges in wavelength from approximately 400 nm (4 x 10^{-7} m) to 700 nm (7 x 10^{-7} m). It is also known as the optical spectrum of light. The wavelength was shown in Table 2.3. The wavelength (which is related to frequency and energy) of the light determines the perceived color. The ranges of these different colors are listed in the table. Some sources vary these ranges pretty drastically, and the boundaries of them are somewhat approximate as they blend into each other. The edges of the visible light spectrum blend into the ultraviolet and infrared levels of radiation.

Table 2.3 The visible light Spectrum

Color	Wavelength (nm)
Red	625-740
Orange	590-625
Yellow	565-590
Green	520-565
Cyan	500-520
Blue	435-500
Violet	380-435

2.11 Dynamic Mechanical Analysis [8]

Dynamic Mechanical Analysis or DMA is a technique to study and characterize material. DMA measures the stiffness and damping properties of material. The polymer is cut and holds by handle. A force which is shown in figure 2.5 is applied to the measurement. The temperature of the sample is changed. When we apply sinusoidal stress (σ) to sample, the material response is strain (ε). The phase lag between the stress and strain is δ. The complex modulus (E^*), storage modulus (E'), loss modulus (E'') and $\tan\delta$ were calculated following equation (2)-(6). The $\tan\delta$ comes from loss modulus divided by storage modulus. Loss modulus is defined as being proportional to the energy dissipated during one loading cycle. Storage modulus represents the stiffness of a viscoelastic material and is proportional to the energy stored during a loading cycle. The phase angle δ is the phase difference between the dynamic stress and the dynamic strain in a viscoelastic material subjected to a sinusoidal oscillation. Figure 2.5 shows DMA profile in which, X axis is temperature and Y axis is Modulus and $\tan\delta$. The material goes through its glass transition. The modulus reduces and the $\tan\delta$ goes through a peak.
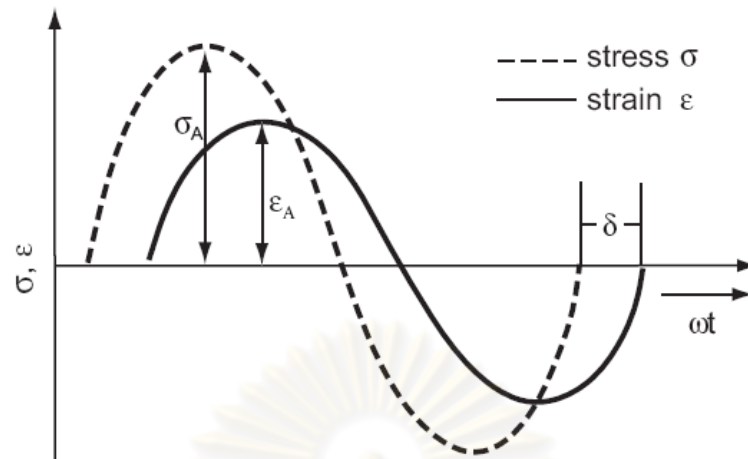
Fig 2.5 Sinusoidal oscillation and response of a linear-viscoelastic material

$$\left|E^*\right| = \frac{\sigma_A}{\varepsilon_A} \tag{2}$$

$$\left|E^*\right| = \sqrt{[E'(\omega)]^2 + [E''(\omega)]^2} \tag{3}$$

$$E'(\omega) = \left|E^*\right| \cos \delta \tag{4}$$

$$E''(\omega) = \left|E^*\right| \sin \delta \tag{5}$$

$$\tan \delta = \frac{E''(\omega)}{E'(\omega)} \tag{6}$$

2.12 Glass transition temperature

The glass transition temperature (Tg) of polymer material is the critical temperature at which the material changes its behavior from being glassy state to being rubbery state. Glassy state means hard and brittle (and therefore relatively easy to break), while rubbery state means elastic and flexible. Usually when the temperature is lower than Tg the polymer chain will be hard to move. On the other hand when temperature is increased until Tg the chain end of polymer will become vibration. If the temperature was increased higher than Tg the polymer will become more flexible (rubbery state). The parameter affects Tg such as chain flexibility, interchain attractive forces and the presence fillers.

2.13 Literature reviews

2.13.1 Investigation synthesis of ZnO

Manzoo and Kim investigated size controls of ZnO particles which were synthesized by gas phase reaction. Zn powder and carbon black were mixed and placed in alumina boat. Argon were used to be carrier gas and oxygen were used to be reaction gas. The shape of ZnO is the effect from Ar flow rate and temperature. When the temperature shape of ZnO was changed from ZnO nanocombs to be ZnO nanowires and ZnO nanorods. Moreover the diameter and size distribution of ZnO increases with increasing in Ar flow rate. In addition to study the effect of ZnO shape ZnO nanowires can show luminescence in visible zone. On the another hand ZnO nanorods and ZnO nanocombs show luminescence in boat UV zone and visible zone. The ZnO nano combs were heat treatment at 800 and 900°C. When heat treatment temperature was increased the luminescence intensity in visible zone was decreased. [9]

Park et al. studied the growth of ZnO nanowires when very small amount of oxygen was used. Zn metal, oxygen gas and nitrogen gas were used in their study experiment. The temperature was varied between 700-1000 °C. The total flow rates entering the reactor were set to 200 ml/min and oxygen concentration were changed. ZnO nanowires became shorter when increasing oxygen concentration. The effects of the temperature were investigated. ZnO nanorod became nanowires and needle when temperature was varied 700, 800 and 900°C respectively. The ZnO nanowires which were synthesized with oxygen content of 1.6 vol% in the temperature range 700-1000 °C were investigated photoluminescence properties. ZnO showed strong peak at ultraviolet region and very week peak at visible region The PL intensity in ultraviolet region decreased when increasing the synthesis temperature. On the contrary the PL intensity in visible region increased when increasing the synthesis temperature.[10]

Gong et al. synthesized ZnO by burning Zn particle in air covered with two firebricks. They obtained two kinds of ZnO. The first one is ZnO tetrapod which has one μm long leg and each leg is measured from the center to its end. Another one is ZnO rod-based tetrapod. It is 60% of the product. The formation process of ZnO tetrapods was proposed. Zn was vaporized under high temperature at atmospheric condition, and then

Zn vapor was oxidized and nucleated in the air. ZnO grows along [0001] direction rapidly. Because [0001] was favorable growth direction in one dimension, the nanorod was grown longer and thicker along with reaction time. When the nanorod diameter grows to larger size than a critical value, some Zn vapor was grown at [1210] and [1010] surfaces. ZnO rod-based tetrapods had strong emission band at 389 nm and weak and broad emission band at 517 nm. The emission at 389 nm was considered near theory value, which came from the recombination of free excitons.[11]

Shen et al. controlled morphologies of ZnO. The influences of Zn vapor, oxidization time and temperature were investigated. The reactor was separated to be evaporation zone and condensation zone. Two types of ZnO tetrapods leg were synthesized. The first one is uniform hexagonal which is the result of kinetically controlled crystal growth along [0001] direction. The second one is hierarchical hexagonal when the thermostatic of ZnO condensation time was longer than 120 min, the ZnO vapor was completely formed in thicker part of leg. The leg morphology of the tetrapod ZnO depended on Zn vapor oxidization temperature and time, as well as the ZnO condensation temperature and time. The increase of the thermostatic ZnO condensation time resulted in the morphology transition of the tetrapod legs from hierarchical hexagonal (HH) to uniform hexagonal (UH) prism. The tetrapod ZnO nanocrystals with uniform hexagonal (UH) legs can only be obtained at relatively higher condensation temperature and longer condensation time. [12]

Ren et al. synthesized ZnO nanowire on zinc substrate at low temperature in the range of the 200 – 400 °C. A pure zinc metal block was polished with sand paper and cleaned by dilute hydrochloric acid and de- ionized water. Zn was placed into ceramic tube which was inserted to a tube furnace. First oxygen gas flow was used 200 standard cubic centimeters per minute (sccm) for 30 min. Next ceramic tube was heated and O_2 flow rate was changed to be 20 sccm. The oxidation reaction between Zn and oxygen were produced and ZnO nanowire was obtained with 20-150 nm and the lengths from several micrometers.

From this research, when a pure zinc metal block was heated, zinc atom at surface can react with oxygen to form a condense oxide film of ZnO. Some tiny oxide crystals will be self catalytically on film to be whiskers or nanowires.[13]

Geng et al. synthesized new shape of ZnO which was sisal shape. They used zinc acetylacetonate as precursor which was placed in quartz tube furnace which has two zones: high temperature zone and low temperature zone. The end of the quartz tube was opened to the atmosphere. Flow rate of Ar was 50 sccm. Zn(acac)2 was vaporized at 150-160 °C and was carried by Ar into higher temperature zone. ZnO nanosisal was glown on silicon substrate at 400-500 °C. The novel sisal- like ZnO nanostructure were several shape which have lengths up to several hundred nanometers and average diameter of 30 nm.

This research supported the method of synthesis ZnO nanoparticles by dividing the reactor in to two zones which can easily be controlled the synthesized parameter. [14]

Chen et al. synthesized tetrapod ZnO nanostructures. ZnO particles were synthesized from Zn powder by vapor phase oxidation method. The temperature, reaction time and flow rate of Ar which was used as carrier gas was varied. ZnO nanoparticle which have three types of tetra pod tip were synthesized. The products can be classified into rod–wire junction, dumbbell-like and cone-like tetrapod. The formation of tetrapod ZnO nanostructures may include two stages: nucleation and growth. The nuclei are octatwins which consist of eight tetrahedral-shaped crystals and the polarities of the twinned crystals are anti-symmetric, and the rods grow from the four [0001] planes. Following nucleation, the nanorods were carried out at high temperature region by carrier gas under the limited oxygen, the second step growth process occurred in layer [0001], and then nanowires were formed at the nanorods. Dumbbell-shaped structures have different growth process, similar to tetrapod with trumpetlike, caused by rich oxygen condition as the kinetics factors which are dominating since the growth rate along the [0001] direction depends on the oxygen partial pressure to a different extent. Their nanodumbbell structures were synthesized in an abundant oxygen condition. In contrast, at very short synthesis time (about 1 min) and lower oxygen supply, the conical structure is formed along the growth direction.[15]

Wu et al. studied structural and optical properties of ZnO nanosaws. The ZnO has a length of about 1-5 µm and diameters of about 100 nm. The raw marteriall is Zn powder and Mg_3N_2 with a weight ratio of 10:1 and place in a ceramic boat in quartz furnace tube. The Ar (200 ml/in) was used as carrier gas. The nanosaw was formed on the

Si substrate. The appearance of diffraction spot [0002] confirms that teeth of nanosaw growth was along the c-axis direction. The Zn powder turned into Zn vapor during the evaporation and formed Zn or ZnO nanostructures. After that the solid ZnO particle were condensed from the droplets. Usually the [0001] direction is the fastest growth direction along on the side of ZnO comb structures. The PL spectra of ZnO nanosaw was measured at room temperature. The ZnO nanosaw showed strong UV peak (3.22 eV) which was near band edge emission and weak green band (1.9-2.8 eV). The strong UV emission and weak green emission in PL spectra indicate that the ZnO nanosaw has good optical quality with few oxygen vacancies. [16]

2.13.2 Investigation of ZnO/PMMA composites

Nowadays several researches try to use the ZnO to be filler in polymer matrix. The properties of nanocomposites can be obtained by imparting the advantage characters of parent elements such as higher thermal stability more than pure polymer, to be a UV shielding capacity and so on.

Lee et al. synthesized nano-ZnO in poly(vinyl alcohol) and poly(ethylene oxide). Nano-ZnO were dispersed in aqueous solutions before added in polymer. The properties of the cast films were optimized by inclusion of 1 wt% ZnO nanoparticles. The addition of 1 wt% ZnO to PVA/PEO blends increases loss modulus, but on the other hand addition of more than 1% ZnO particles decreases loss modulus. At higher nanoparticles loading the particles tend to agglomerate, to an increasing extent as the nanoparticles content increases, and agglomeration of the oxide particles has a detrimental effect on film properties.[17]

Hung and Whang studied effect of surface stabilization on luminescent characteristics in ZnO/poly(hydroxyethyl methacrylate) nanohybrid films. They synthesized 2-3 nanometer sized ZnO by solution method and use a 3-(Trimethoxysilyl)propylmethacrylate (TPM) to be stabilizing agent. TPM-modified nanoparticles have better dispensability and controllable luminescent properties. The size of ZnO was in the range of 2.2-3.2 nm. The 2.2 nm of ZnO/PHDMA composite show

maximum wavelength at 530 nm and the 3.2 nm of ZnO/PHDMA composite show maximum wavelength at 515 nm. In case of using TPM to the 2.2 nm of ZnO /PHDMA composite show maximum wavelength at 510 nm and the 3.2 nm of ZnO PHDMA composite show maximum wavelength at 453 nm. The dispersion of ZnO in polymer matrix were investigated by SEM. TPM-surfaced modification really permits superior stability and dispensability of ZnO nanoparticles into the polymer matrix compared to the unmodified ZnO nanoparticles, probably because of the covalent attachment between nanoparticles and polymers.[18]

Tang et al. investigate method to prevent agglomeration of ZnO particle by using copolymer, polymethyl methacrylate (PMMA) and polymethacrylic acid (PMAA). They use insitu emulsion polymerization under nitrogen atmosphere. ZnO (50nm) is dispersed by ultrasonic and filled into mixture of monomer, initiator and additive at 75 °C and left for 8 h. ZnO are formed to interact with copolymer before blended with PVC to prepare nanocomposite. It was found that ZnO coated by copolymer could exhibit better dispersion stability than uncoated ZnO. TGA analysis indicates that nanocomposite of coated ZnO and PVC could exhibit higher thermal stability than pure PVC.[19]

Hu et al. studied visocoelastic properties of silica and polymethyl methacrylate (PMMA) composite which were prepared by a bulk polymerization technique. The silica powder was dispersed throughout the MMA monomer under sonification after that the mixture was warmed to 80°c for 30 min; it was cooled to room temperature to cast by using 3 mm PVC packing. Finally, the mixture was polymerized at 55°C for another 12 h in a water bath and cured at 110 ^{o}C for an hour. They found that the thermal characteristics of these composites were also enhanced by the incorporation silica into the PMMA. The T_g of these composites increased with the silica content. The degradation temperature at 10% weight loss was also approximately 30°C higher than that of pristine PMMA. [20]

CHAPTER III

EXPERIMENTAL

The experimental procedure of this work was separated into two parts as follow:

synthesis of zinc oxide nanoparticles and preparation of ZnO/PMMA composite

3.1 Material

Zn particles which were bought from Sigma-Aldrich were used to be raw matirial. The purity of Zinc is 99.999%. Figure 3.1 shows that Zn particles were investigated by SEM. The morphology of Zn particle is sphere and size is smaller than 10 micrometers.
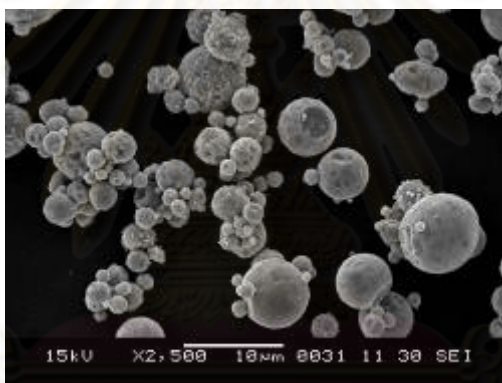
Figure 3.1 SEM image of Zn raw material

The PMMA/ZnO composite films were prepared from ZnO particles which were purchased from Wako Pure Chemical Industries. ZnO commercial A and commercial B were purchased from the company. PMMA was obtained from Kuraray Co.,LTD. Figure 3.2 (a) shows typical SEM image of ZnO commercial A. The average size is 1.9 micrometer. Figure 3.2(b) shows ZnO commercial B whose average size is 2.3 micrometer. Figure 3.2 (c) shows ZnO which were synthesized by gas phase reaction. The Zn particles were evaporated at 900 °C. Air and nitrogen were used to be reaction and carrier gas. Both gases were controlled flow rate at 1 l/min. The ZnO particles were collected by filter holder which is polymer membrane. The ZnO particles which was synthesized by gas phase reaction have a micro meter size and the shape is a mutipods whose its tip is in nanometer size.
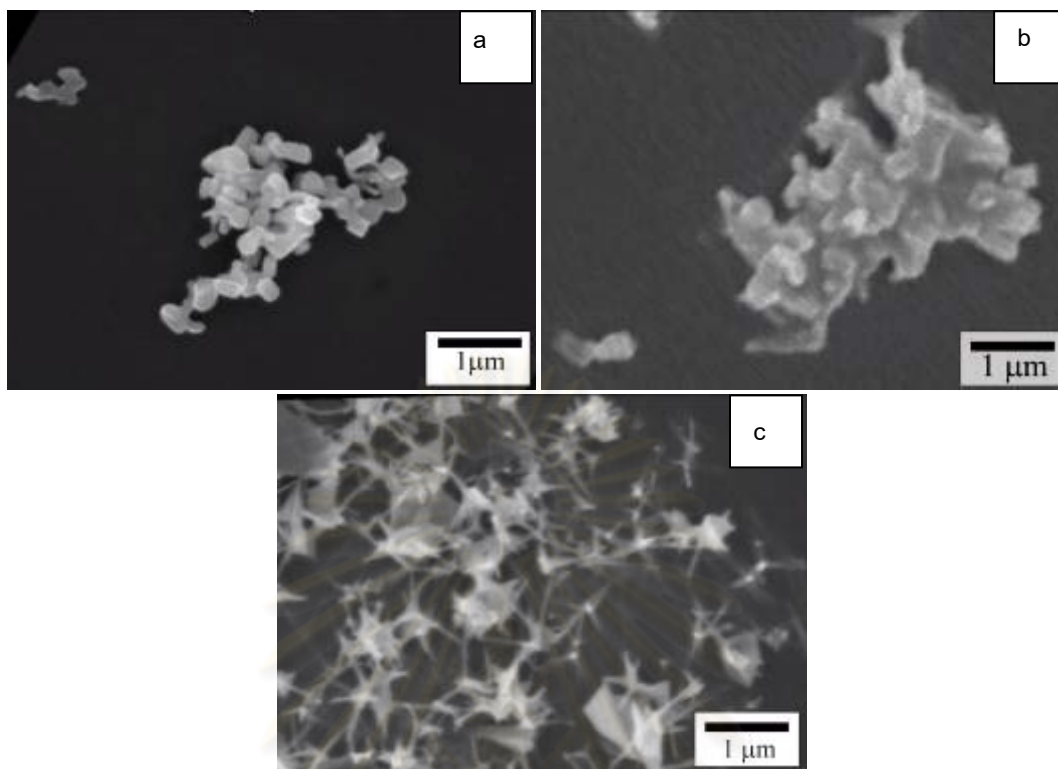
Figure 3.2 (a) ZnO commercial A, (b) ZnO commercial B and (c) ZnO synthesized by gas phase reaction. Using oxygen flow rate at 1 l/min, nitrogen flow rate at 1 l/min, temperature 900°C

3.2 Experimental procedure

3.2.1 Synthesis of Zinc Oxide nanoparticles

ZnO particle were fabricated in a horizontal quartz tube furnace by gas phase reaction without catalyst. The gas phase reaction process was showen in figure 3.2. The quartz tube reactor has 60 cm in length 4.3 cm in diameter. The electrical furnace has 30 cm in length. The Zn particle 2 g was loaded into alumina boat. Nitrogen which was varied between 1000-3000 ml/min was used as carrier gas. Then Oxygen which was varied between 20-60 ml/min was used a reaction gas. The temperature of reaction was 700 °C. When the reactor was heated until 700 °C the boat was moved into the reactor. The reaction time was 15 minute. After the growth process, the reactor furnaces were allowed to cool down at ambient temperature. The ZnO particles deposited on quartz tube reactor and flask. After that the ZnO particle were scraped and investigated by SEM.
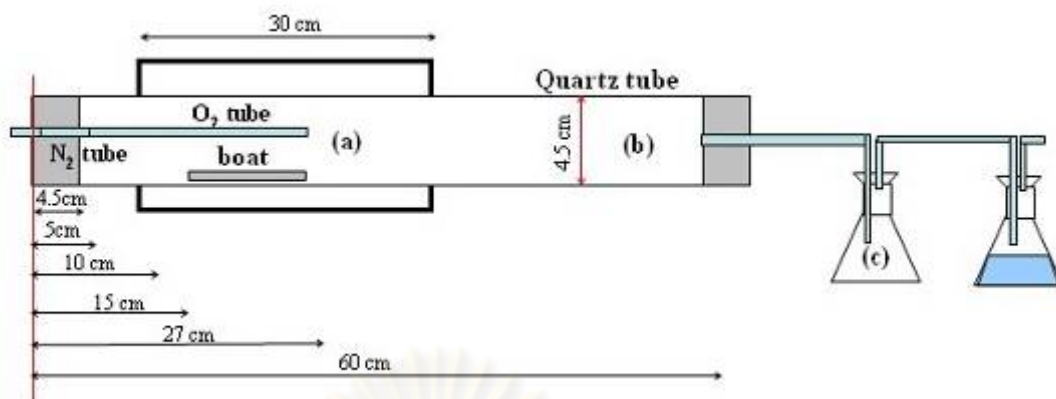
Figure 3.3 Experimental set up for synthesized ZnO nanoparticles by gas phase reaction process

The investigation of ZnO particles by SEM found that the particle which was deposited on quartz tube and flask had micro size. The ZnO nanoparticles were presumed that it was not deposited on quartz tube and flask. It was carried to environment by nitrogen gas. Therefore the system which was used to synthesize ZnO particle was improved the collecting particle method by useing filter and vacuum pump as shown in figure 3.4. The quartz tube reactor has 120 cm in length 4.5 cm in diameter. The Zn particle 2 g was loaded into alumina boat which was placed in middle of furnace. Nitrogen which was varied between 1000 and 1500 ml/min was used as carrier gas. Then oxygen which was varied 20, 40 and 60 ml/min was used as reaction gas. The temperatures of reaction were 600 and 700 °C. When the temperature was varied at 600 or 700 °C ZnO particles were collected at the outlet of the reactor by filter. The filter holder was shown in figure 3.5. The vacuum pump was set flow rate constant at 1000 ml/min After the growth process, the reactor furnaces were allowed to cool down at ambient temperature.
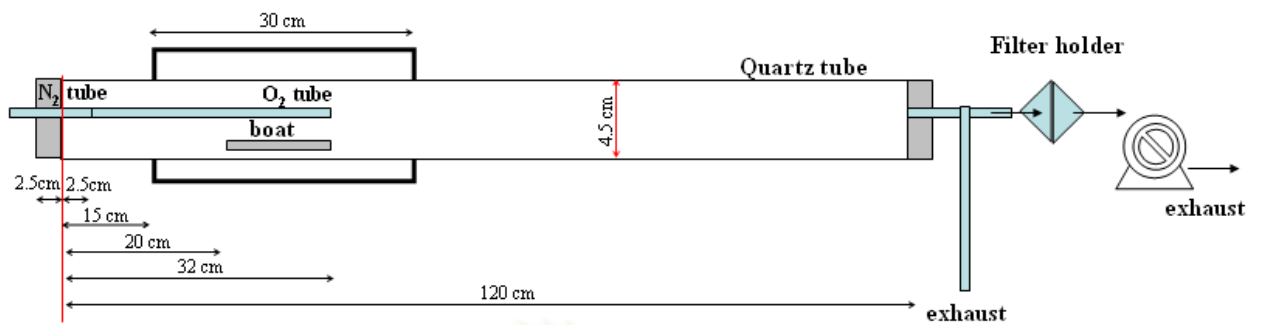
Figure 3.4 Experimental set up for synthesized ZnO nanoparticles by gas phase reaction process after improved collecting particle method.

Figure 3.5 Filter holder

3.2.2 The instrument which was used to prepare ZnO/PMMA composite

a) Two roll mill

The PMMA and ZnO particles were mixed for 10 min at 200°C using a two-roll mill as show in figure 3.6. The front and back roll of two roll mill speed is 16 and 8 round per minute respectively.

Figure 3.6 Two roll mill

b) Hot press

The mixed materials were subjected to a compression molding to prepare 0.2 mm thick films. The hot press was shown in figure 3.7. The operating condition of the compression molding machine was 200 °C and 100 MPa. The specimens was immersed in 0°C water to cool it down.

Figure 3.7 Hot press

3.3 Analytical instruments

The instruments used to characterize the properties of synthesized ZnO are XRD (Bruker AXS model D8 discover), SEM (Hitachi, S 4500 and JEOL model JSM-6400) and TEM (JEOL model JEM-2100) for finding the morphology and size, phase of ZnO particle while optical and mechanical properties of composite films were investigated by UV/VIS spectrophotometer (JASCO, V570), Photoluminescence (JASCO FP-6200) and Dynamic mechanical analysis (PYRIS Diamond DMA)

3.3.1 X-Ray Diffraction (XRD)

The XRD (Bruker AXS model D8 discover) in Figure 3.8 was used to analyze phase of the investigated ZnO particle.

Figure 3.8 X-Ray Diffraction

3.3.2 Scanning Electron Microscopy (SEM)

Morphology and size of ZnO particles were investigated by SEM (Hitachi, S 4500 and JEOL model JSM-6400). ZnO particle were dispersed in ethanol and used ultrasonic treatment with the sufficient time (15 min) for ensuring its uniform dispersion. The mixed of ZnO in ethanol were dropped on the glass slide and heated to evaporate ethanol. The shape and size of ZnO were observed by SEM images. Then the sample was placed directly onto a conductive gold coated microscope grid. The specimens were loaded into a sample chamber, and observations were immediately started using image catcher scanner for taking the photos. A photo of the Scanning Electron Microscopy (SEM) machine is shown in Figure 3.9

Figure 3.9. Scanning Electron Microscopy

3.3.3 UV-Vis spectrophotometer (UV-vis)

UV/VIS spectrophotometer (JASCO, V570) in figure 3.11 was used to measure the adsorption and % transparency of ZnO/PMMA film. Figure 3.12 is film holder in UV/VIS spectrophotometer. The scanning speed was 400 nm/min in the range of 200-800 nm wavelengths.

Figure 3.10 UV/VIS spectrophotometer

Figure 3.11 Film holder in UV/VIS spectrophotometer

3.3.4 Photoluminescence (PL)

The fluorescence spectra were determined with a JASCO FP-6200 spectrophotometer. Figure 3.12 shows the photoluminescence spectrophotometer used in this work. The ZnO powder and Composite film were scanned in the range of 350-600 nm wavelengths. The excitation was 325 nm.

Figure 3.12 Photoluminescence spectrophotometer

3.3.5 Dynamic mechanical analysis (DMA)

Dynamic mechanical analysis of the specimens was performed using a PYRIS Diamond DMA with a heating rate of 2 °C/min and frequency of 10 Hz. The DMA instrument was showed in figure 3.13. The nanocomposites of film samples were cut into rectangular shapes 20mm×10mm×0.50mm

Figure 3.13 Dynamic mechanical analysis

CHAPTER IV

RESULTS AND DISCUSSION

As already mentioned in previous chapters, this research has set its aim to study effect of parameters on the morphology of ZnO nanoparticles synthesized from gas phase reaction method. Effect of gas flow rate and collecting method on the morphologies and size of synthesized ZnO nanoparticles were experimentally investigated and then reported and discussed at the beginning part of this chapter. Then the preparation of PMMA/ZnO composite with respect to the compounding conditions and their photoluminescent behavior would be also reported and discussed.

4.1 Investigation of synthesizing parameter on characteristics of ZnO nanoparticles

The schematic diagram of experimental set up employed for synthesizing ZnO is shown in figure 4.1. After the temperature was increased to a certain set point (600 or 700 °C) an alumina boat containing zinc particles was inserted to the designated position in the reactor. Then oxygen and nitrogen gas were fed in to the system. Zn vapor would undergo the oxidation reaction with oxygen and turned to ZnO particle which deposited on the inner surface of the quartz tube reactor. In each experiment, the system was left for 15 minutes after introducing O_2. ZnO product was mainly collected from the deposit of the reactor wall at 3 positions which are (a), (b) and (c) as shown in figure 4.1. The (a) position which was located within the furnace was remarked as "hot zone" in which temperature range was 400-620 °C. The (b) position at the end of tube was called as "cold zone" in which temperature range was 100-400 °C and the (c) position was "trapping bottle zone" in which temperature range was ambient temperature. Those collected products were analyzed using SEM and image analyses for identifying their morphology and size distribution.

4.1.1 Effect of oxygen flow rate on ZnO morphologies

The ZnO particles which were collected from deposits within the quartz tube reactor and the trapping flask were investigated by SEM. Before SEM analysis, the ZnO particles were dispersed in ethanol and subjected to ultrasonication for 30 min and then being heated to vaporize ethanol out of the specimen.

Figure 4.2 shows typical images of ZnO particles synthesized under different conditions of O_2 concentrations. With constant N_2 flow rate of 1000 ml/min and constant temperature of 700°C, some ZnO tetrapods could be abundantly obtained with the O_2 flow rate of 20 ml/min. Moreover, the smallest size of ZnO tetrapods was mainly obtained in the "hot zone" (Figure 4.2a). Typical tetrapods possess symmetric pods with a length of 500 nm and diameter of 130 nm.

In case of 30 ml/min O_2 flow rate, ZnO nanoparticles synthesized at the same temperature and N_2 flow rate exhibited significantly different morphology. It could be observed from Figure 4.2b that at the center of each tetrapod there existed a core which extended in a certain direction. The growing of the core was more enhanced by the further increase in O_2 concentration. With the O_2 flow rate of 70 ml/min, the synthesized ZnO particles turned into a plate-like morphology. An increase in oxygen flow rate affects to increase ZnO concentration. However the exit of reactor was very small so that the ZnO particle could not release and flow back to reactor, resulting in supersaturation in reactor. For this reason, the shape of ZnO changed from tetrapod to plate-like. Chen et al synthesized ZnO by vapor deposition method. The higher supersaturation of the Zn vapor and higher oxygen partial pressure led to the formation of the ZnO nanotetrapods. Zn reacted with oxygen in vapor to from small ZnO particle, and the ZnO particles were deposited on the inner wall of the quartz tube. [27]
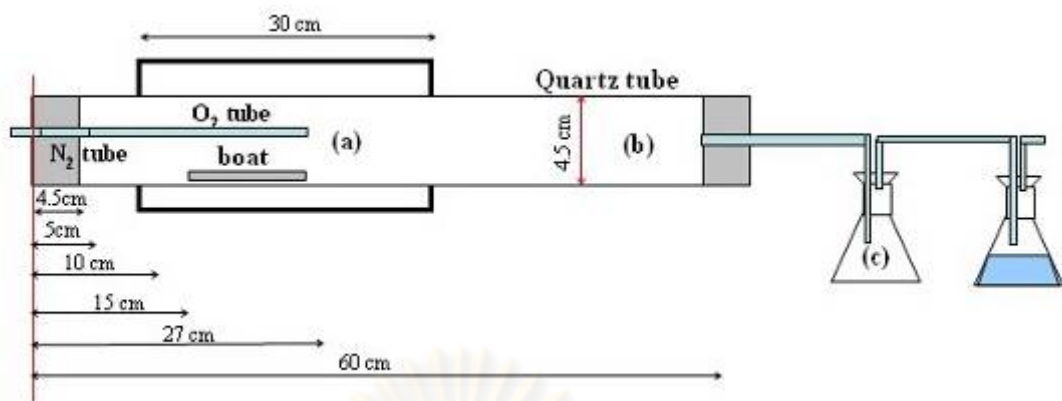
Figure 4.1 Experimental apparatus for ZnO synthesis
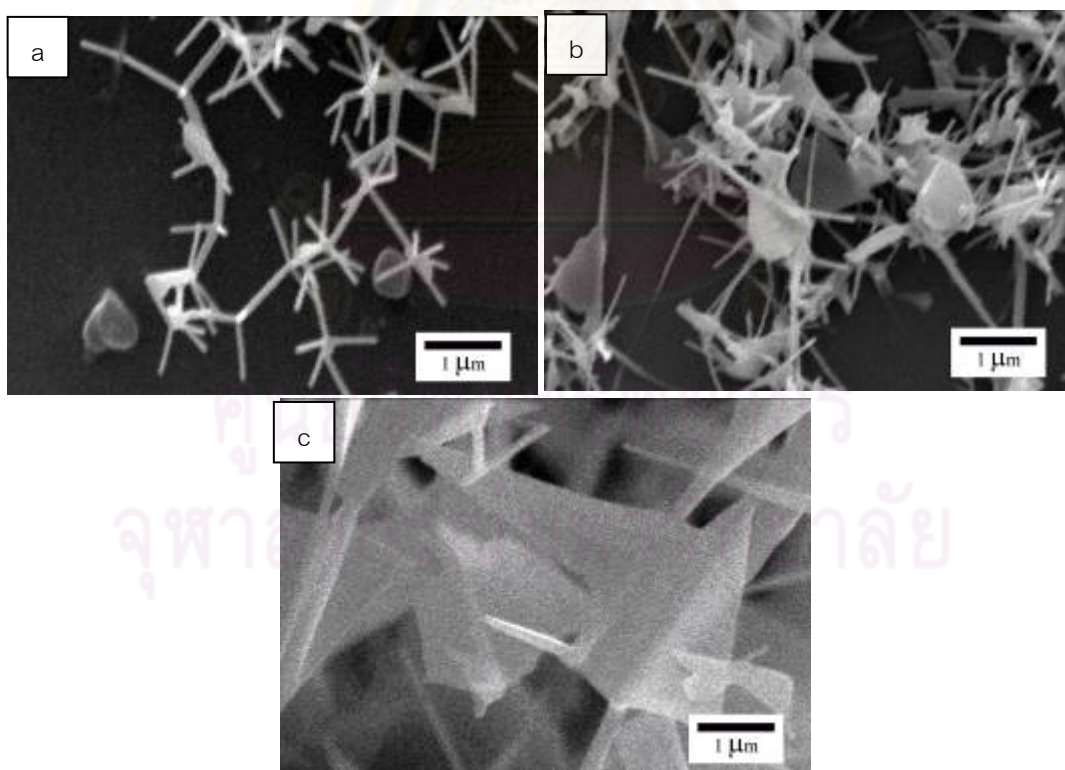
Figure 4.2 SEM micrographs of ZnO particle in hot zone at temperature 700° C by varying oxygen flow rate (a) 20 ml/min, (b) 30 ml/min and (c) 70 ml/min, with nitrogen flow rate 1000 ml/min

4.1.2   Effect of flying distance on ZnO morphologies

Figures 4.2- 4.4 illustrate ZnO particles which were synthesized using O_2 flow rate at 20, 30 and 70 ml/min and N_2 flow rate at 1000 ml/min at 700°C and then collected at three different positions, namely hot zone, cold zone and trapping bottle zone. Based on figure 4.3a the synthesized ZnO tetrapods which were collected in the cold zone had longer length than those collected in the hot zone (figure 4.2a). In addition, the ZnO particles flying to the trapping bottle (Figure 4.4a) exhibited multi-pod morphology with the same pod length. Regarding to these results, it should be noted that with longer time of flight, ZnO tetrapods could grow along the pod direction and finally coalesce with other tetrapods to form multi-pod particles after the growth was terminated.

Figures 4.2c, 4.3b and 4.4c illustrate that under the high concentration of O_2, ZnO particle obtained at any zone would have the core which could grow faster than their pods. This result would be attributed to the sufficient supply of O_2 which in turn resulted in the fast growth of ZnO in the direction of their core.
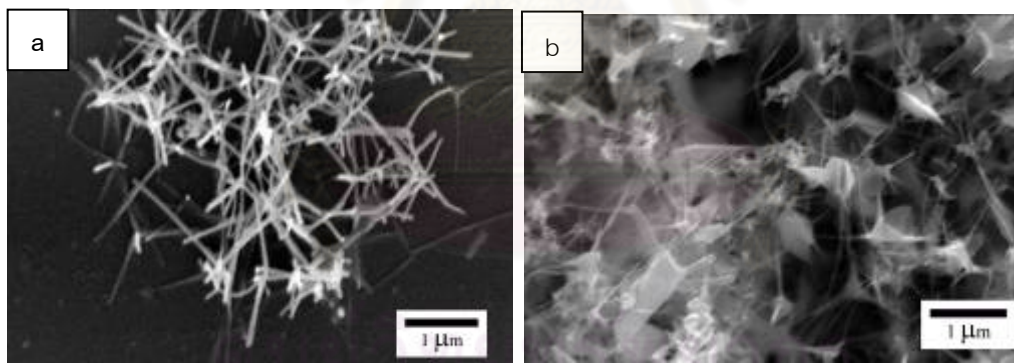
Figure 4.3 SEM micrographs of ZnO particle in cold zone at temperature 700° C   by varying oxygen (a) 20 ml/min, (b) 70 ml/min, with nitrogen flow rate 1000 ml/min
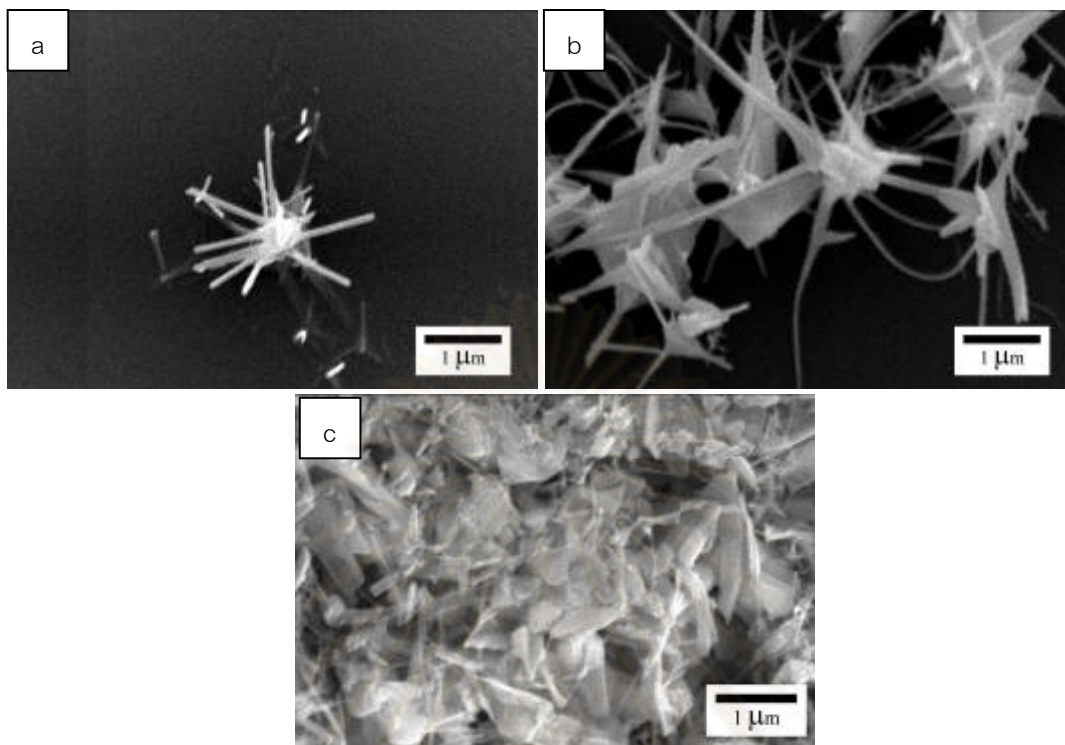
Figure 4.4 SEM micrographs of ZnO particle in trapping bottle at temperature 700° C by varying oxygen (a) 20 ml/min, (b) 30 ml/min and (c) 70 ml/min, with nitrogen flow rate 1000 ml/min

When the sample collecting distance was far from furnace the condensation time of ZnO was increased. Shen et al. found that leg morphology of the tetrapod ZnO effect from the ZnO condensation temperature and time. The increase of ZnO condensation time results in the morphology of tetrapod legs from hierarchical hexagonal to uniform hexagonal prism [28]. It should be noted that with the previous configuration of the quartz tube reactor, only few amount of ZnO products could be collected in each experiment. This would be resulted from the escape of ZnO fine particles though the trapping bottle was employed. In order to improve the collection efficiency, a set of dust collector with a glass fiber filter was connected to the exit of the quartz tube reactor as illustrated in figure 4.5.
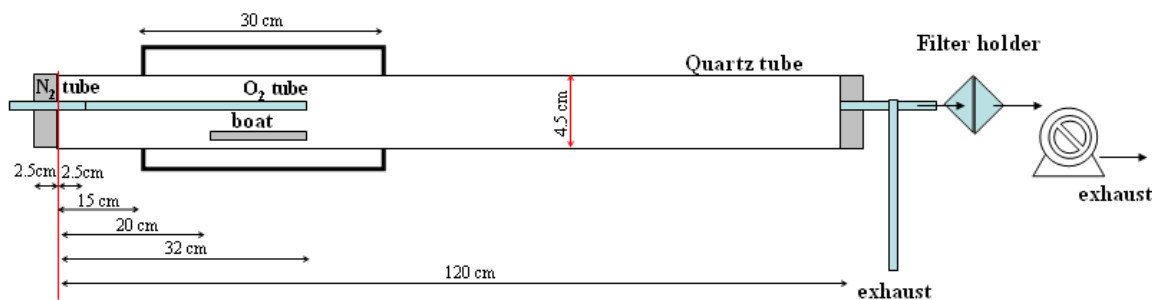
Figure 4.5 Experimental apparatus for synthesis ZnO with improving collection method for synthesized ZnO nanoparticles.

4.1.3   Effect of nitrogen flow rate on ZnO morphology

Nitrogen flow rate were varied in the range of 1000, 1500 and 3000 ml/min with constant oxygen flow rate at 20 ml/min. Nitrogen flow rate was limited at 3000 ml/min because when nitrogen flow rate was more than 3000 ml/min it affects the mixing of Zn vapor and ZnO vapor which bring decreasing of ZnO yield. The ZnO particles collected on glass filters were characterized by SEM analysis. Figure 4.6 shows that morphologies of ZnO nanoparticles depend on nitrogen flow rate. When the nitrogen flow rate was increased the size of ZnO particles became slightly decreased. Higher agglomeration could be observed when the flow rate of oxygen was increased from 20 to 60 ml/min. Based on particle size analysis using an image processing method, figure 4.7 reveals that the nitrogen flow rate of 3000 ml/min would result in the ZnO particles with the smallest average size. This result would be ascribed to the fact that with the higher nitrogen flow rate the partial pressure of oxygen would become lower due to the dilution effect. Therefore, lower amount of ZnO would be obtained from the oxidation reaction, leading to formation of ZnO fine particles which become more easily to agglomerate.

Figure 4.6 SEM micrographs of ZnO particle on glass fiber filter at temperature 700° C by varying nitrogen (a) 1000 ml/min, (b) 1500 ml/min, and (c) 3000 ml/min with oxygen flow rate 20 ml/min
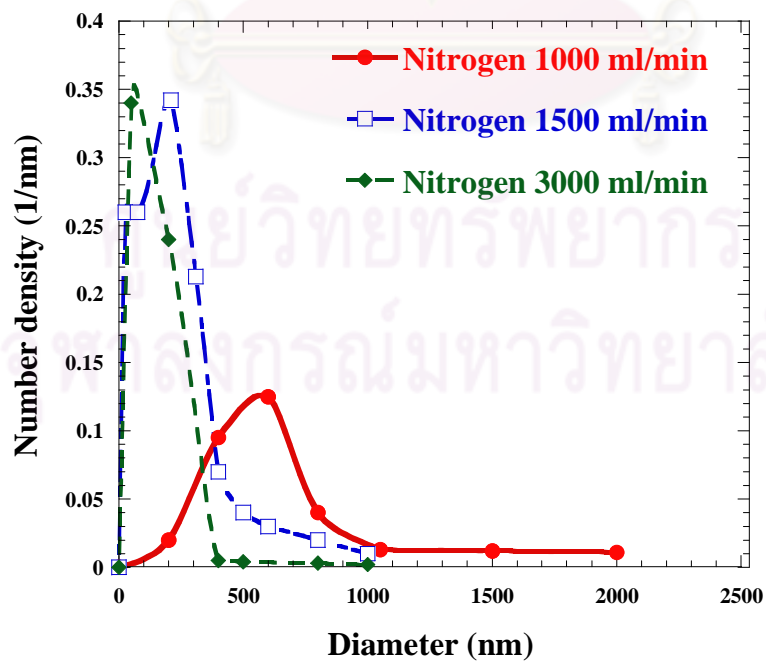
Figure 4.7 Particle size distributions of ZnO nanoparticles by varying nitrogen flow rate with constant oxygen flow rate at 20 ml/min

4.1.4 Effect of oxygen flow rate with the improved collecting method

As mentioned above, the sufficient amount of ZnO particles could be obtained with the reactor equipped with the improved collecting tool. This would be an important issue for repeatable investigation of preparation of PMMA/ZnO composite. Therefore, the effect of oxygen flow rate was re-examined again because it is known as the crucial parameter for controlling the synthesis of ZnO particles.

In this part, the effect of oxygen flow rate was again examined by changing from 20, 40 and 60 ml/min and the nitrogen flow rate was fixed at 1000 ml/min. The temperature was optimized at 600°C based on pervious investigation [26]. SEM micrographs shown in figure 4.8 reveal that when the oxygen flow rate of 20 and 40 ml/min was introduced into the system, the synthesized ZnO nanoparticles exhibited nearly spherical shape with submicron size. When the oxygen flow rate was increased to 60 ml/min, the ZnO particle with short pod could be obtained. Figure 4.9 illustrates ZnO particles which were synthesized with higher nitrogen flow rate of 1500 ml/min. Similar tendency of the morphology of the synthesized ZnO particles could be observed. However, due to the effect of oxygen dilution, the particle size analyses of those particles obtained from the conditions of different nitrogen flow rate illustrates that the lower oxygen supply would provide the smaller size of ZnO particles as shown in figures 4.10 and 4.11.

Regarding to the effect of oxygen flow rate on the size distribution of the synthesized ZnO particles, it could be observed from either figure 4.10 or 4.11 that the higher oxygen flow rate would provide the synthesized ZnO particles with larger size. This result would also be attributed to the increase in the formation of ZnO regarding to the increased oxygen partial pressure, resulting in the faster growth of ZnO particles.

Based on ideal gas assumption, it could be verified that the partial pressure of oxygen would be changed regarding to both nitrogen and oxygen flow rate. The calculated results of oxygen partial pressure regarding to the gas flow rate is depicted in figure 4.12. It was found that when the partial pressure of oxygen was between 0.0132 and 0.034 atm the synthesized ZnO particles had nearly spherical shape. However, when the partial pressure of oxygen was in a range of 0.034 to 0.056 atm, the particle exhibited short leg morphology.

Figure 4.8 SEM micrographs of ZnO particle on glass fiber filter at temperature 600° C by varying oxygen (a) 20 ml/min, (b) 40 ml/min, and (c) 60 ml/min with nitrogen flow rate 1000 ml/min
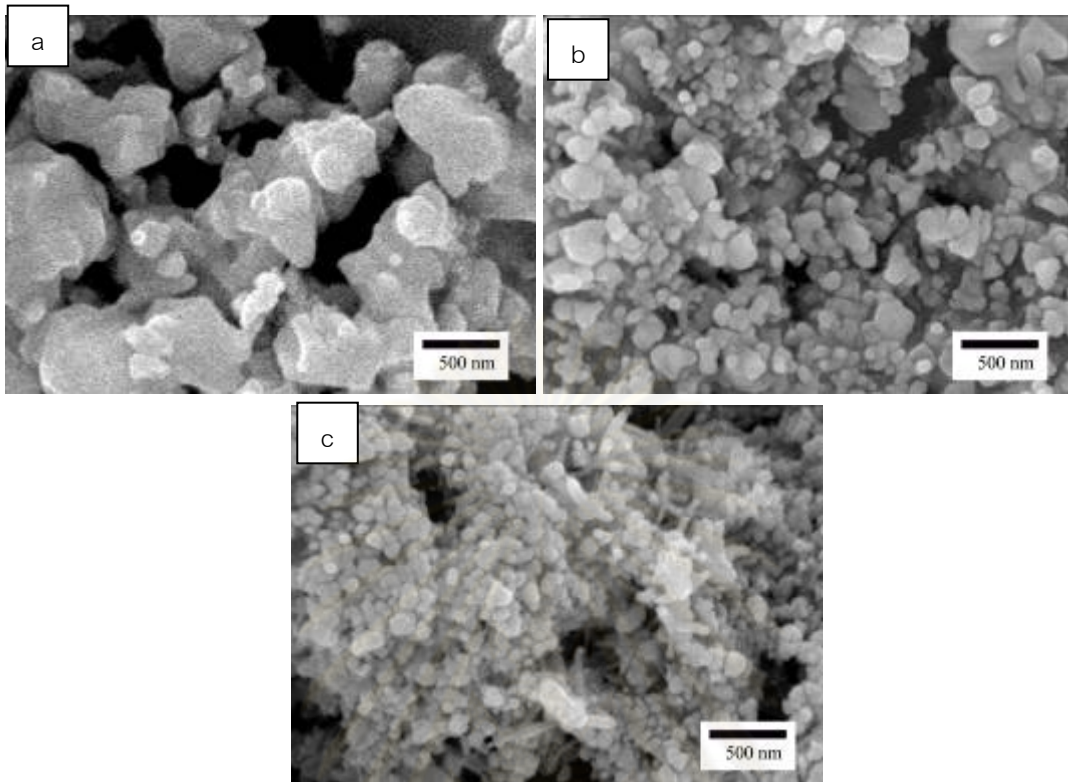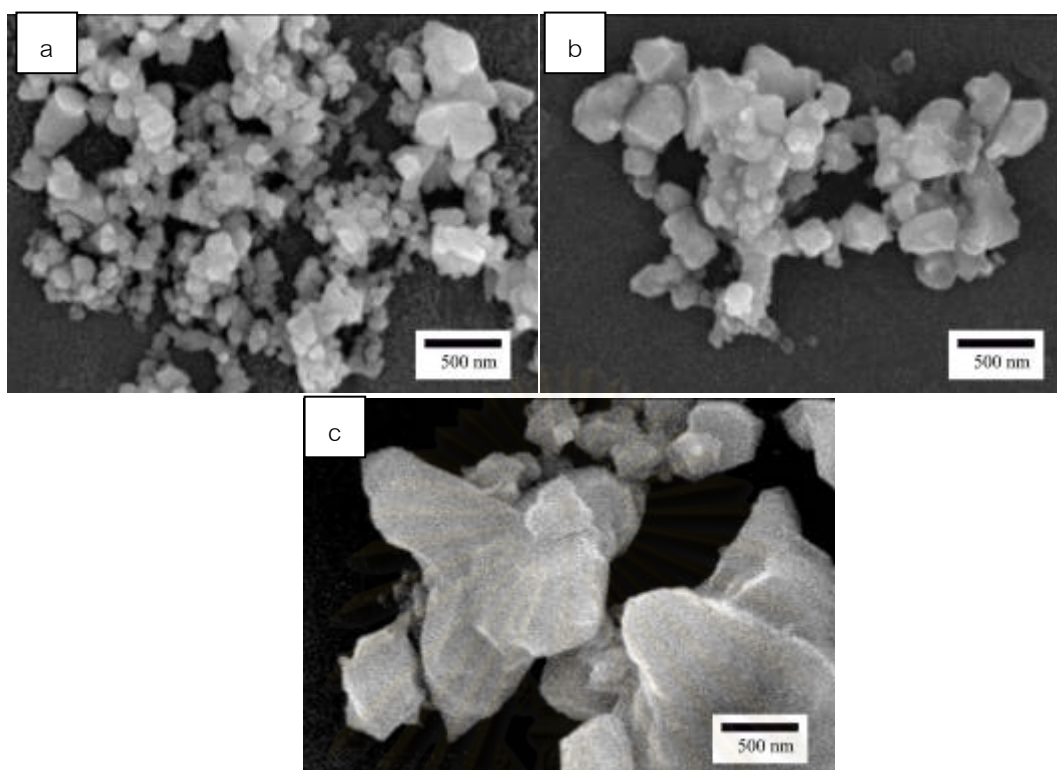
Figure 4.9 SEM micrographs of ZnO particle on glass fiber filter at temperature 600° C by varying oxygen (a) 20 ml/min, (b) 40 ml/min, and (c) 60 ml/min with nitrogen flow rate 1500 ml/min
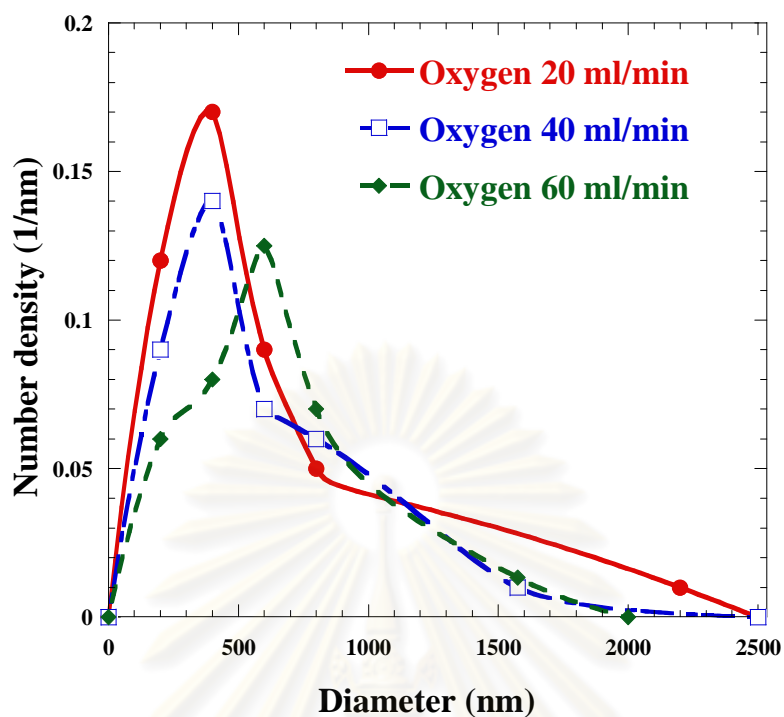
Figure 4.10 Particle size distribution of ZnO nanoparticle by varying oxygen flow rate with constant nitrogen flow rate at 1000 ml/min
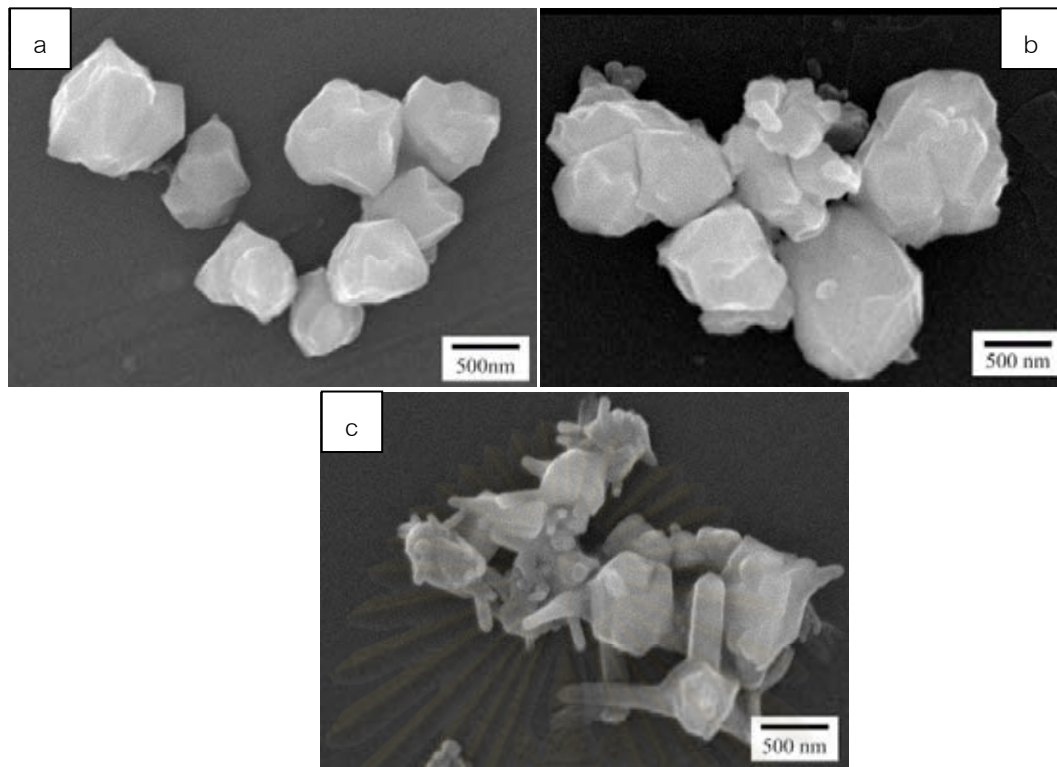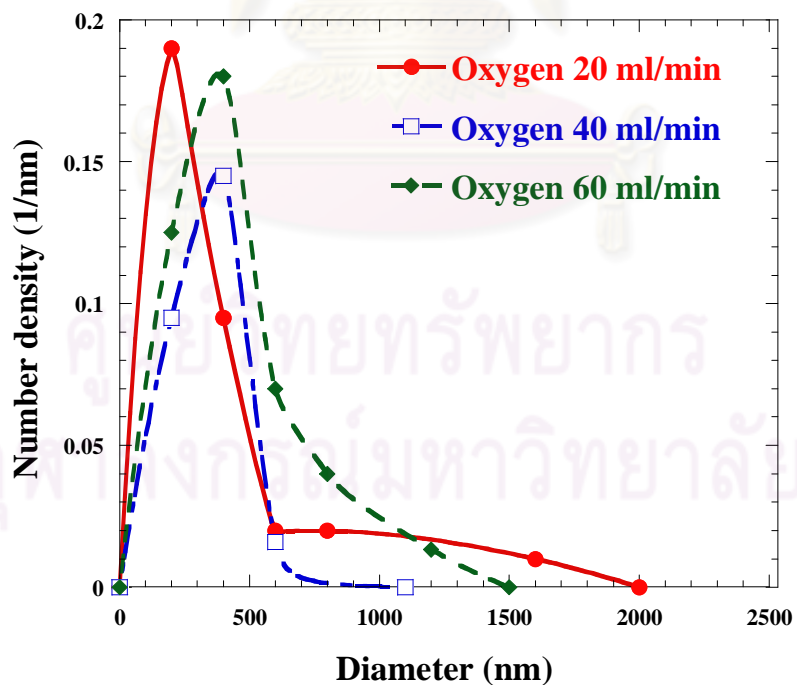

Figure 4.11 Particle size distribution of ZnO nanoparticle by varying oxygen flow rate with constant nitrogen flow rate at 1500 ml/min
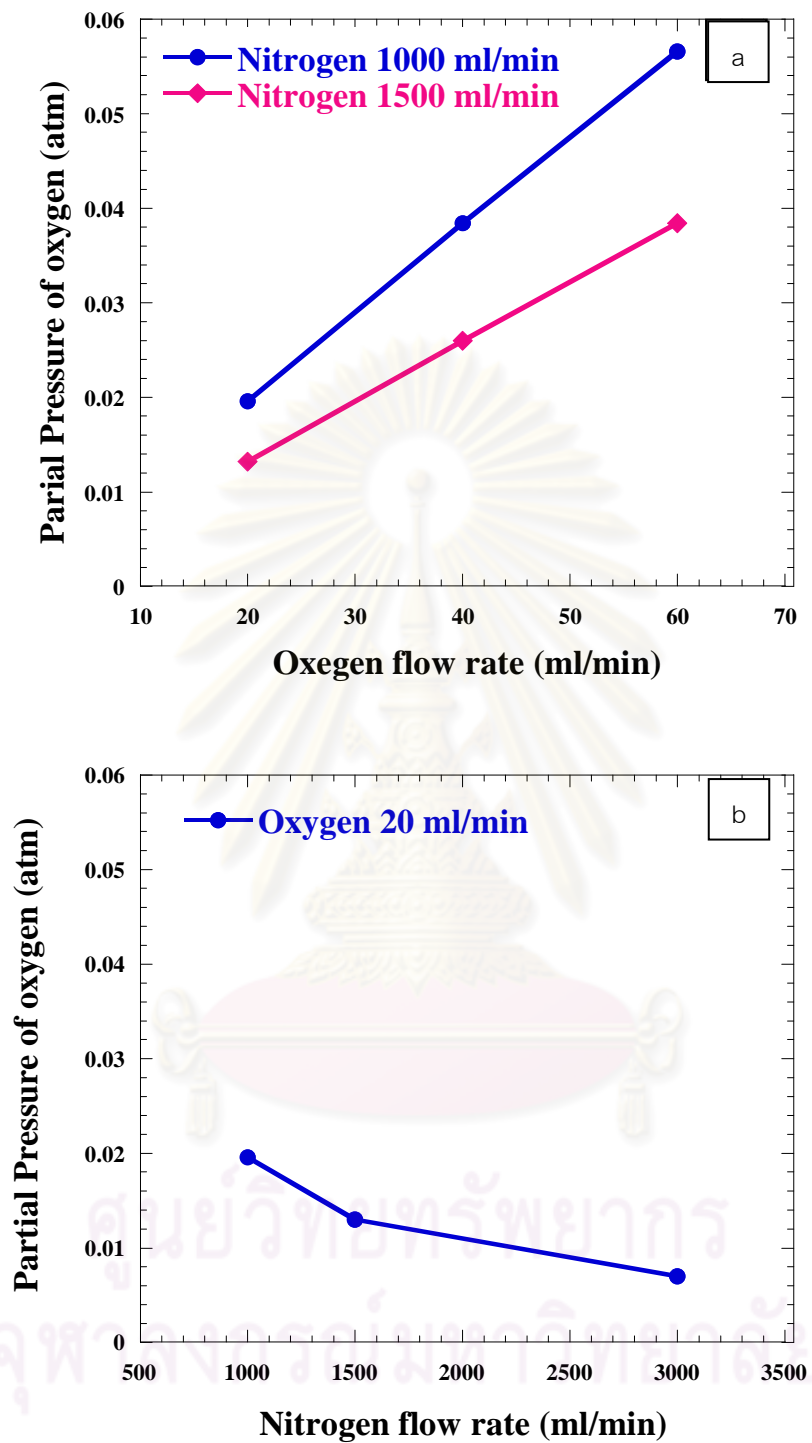
Figure 4.12 Partial pressure of oxygen by varying nitrogen and oxygen flow rate, (a) vary nitrogen flow rate, (b) vary oxygen flow rate

4.2 Properties of ZnO particle which was combined with PMMA

There are 3 types of ZnO particle which were mixed with PMMA. The first and the second type which were purchased from company were called "commercial ZnO A" and "commercial ZnO B". The morphology of ZnO commecial was nearly spherical shape. The third type of ZnO was synthesized by gas phase reaction. The tetrapod ZnO morphology was interested in combine with PMMA matrix. The Zn particles were evaporated at 900 °C. Air and Nitrogen were used to be reaction and carried gas. Both gases were controlled flow rate at 1 l/min. ZnO was synthesized by gas phase reaction were called "ZnO synthesized by gas phase reaction".

4.2.1 Crystalline structure of ZnO particle

Figure 4.13 shows the X-ray diffraction (XRD) pattern of commercial ZnO and ZnO which was synthesized by gas phase reaction. The main peaks appear at 31.9, 34.4 and 36.4 that are typical diffraction peaks from hexagonal ZnO planes of (100), (002) and (101), respectively. As indexed in figure 4.13 all other peaks also match the hexagonal ZnO structure with lattice constants of a = 3.250 Å and c = 5.207 Å. This indicates that the commercial ZnO and ZnO which was synthesized by gas phase reaction are composed of wurtzite structural ZnO. From XRD the average size of ZnO particles can be calculated by using the Scherrer's formula. The estimated average size values are 16, 36 and 27 nm for the commercial ZnO A, commercial ZnO B and ZnO by gas phase reaction, respectively.
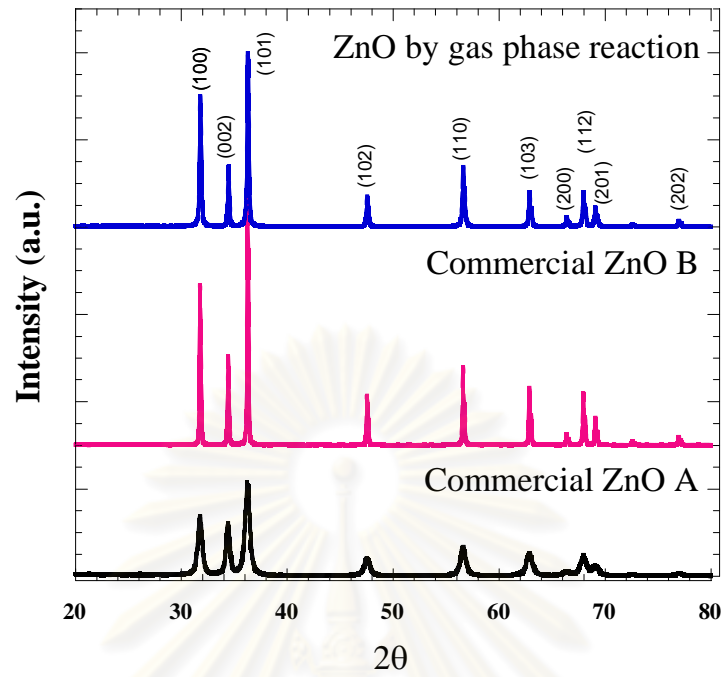
Figure 4.13 XRD patterns of ZnO particles

4.2.2 Particle size distribution of ZnO nanoparticle

Figure 4.14 shows particle size distribution of all ZnO nanoparticle. Almost all commercial ZnO A and ZnO which was synthesized by gas phase reactions had particle size in sub micrometer range (100-1000 nm) which was much smaller than commercial ZnO B. The size of ZnO particles which were synthesized by gas phase reaction were measured at their core. The tip of ZnO particle was about 50-100 nm.
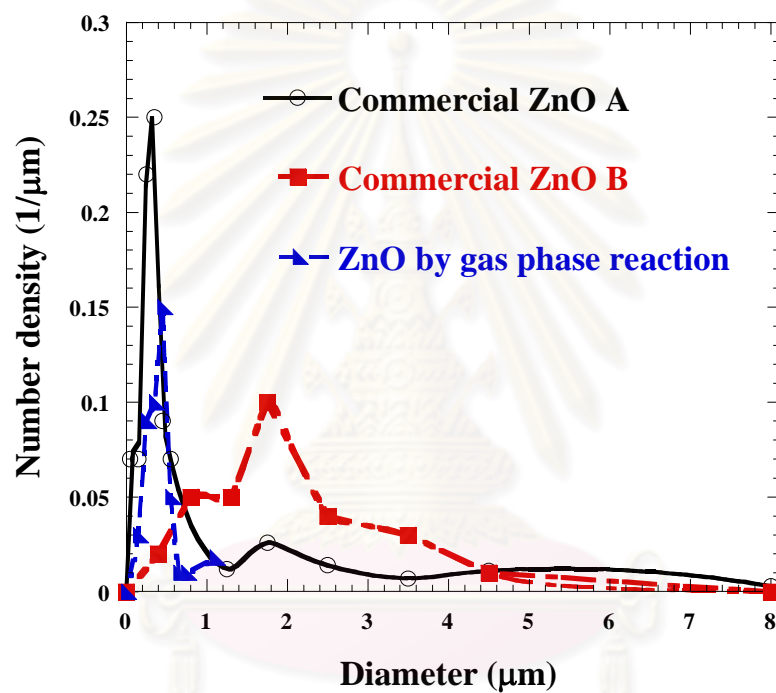
Figure 4.14 Particle size distribution of ZnO nanoparticle by varying type of ZnO

4.2.3 Optical properties of ZnO particles

ZnO particles were dispersed in ethanol and subjected to ultrasonication for 30 minute before investigated by UV/VIS spectrophotometer and luminescence spectrometer. In figure 4.13 ZnO in ethanol were characterized by UV/VIS spectrophotometer. The absorption range is 200-800 nm. The absorption intensity of commercial ZnO A in ethanol is 2 and 1 time when compare with commercial ZnO B and ZnO which was synthesized by gas phase reaction.

ZnO particles in ethanol were studied photoluminescence spectrum by fixing excitation wavelength at 325 nm. The light emissions of ZnO particle in ethanol were shown in Figure 4.16. Commercial ZnO A showed a weak curve at 370- 400. Then Commercial ZnO B showed sharp luminescence peak at 385 nm and weak curve at 408- 580 nm. In case of ZnO which was synthesized by gas phase reaction, It showed strong peak at 380 nm and curve at 405 -580 nm. Commercial ZnO B and ZnO which was synthesized by gas phase reaction, showed two distinct peak's i.e. one peak at UV region and one broad green band at visible region. The UV emission peak at about 380 nm is originated from exitonic corresponding to the band-edge emission of ZnO. The broad green band is attributed to the recombination of a photogenerated hole with an electron occupied at an oxygen vacancy. [22]
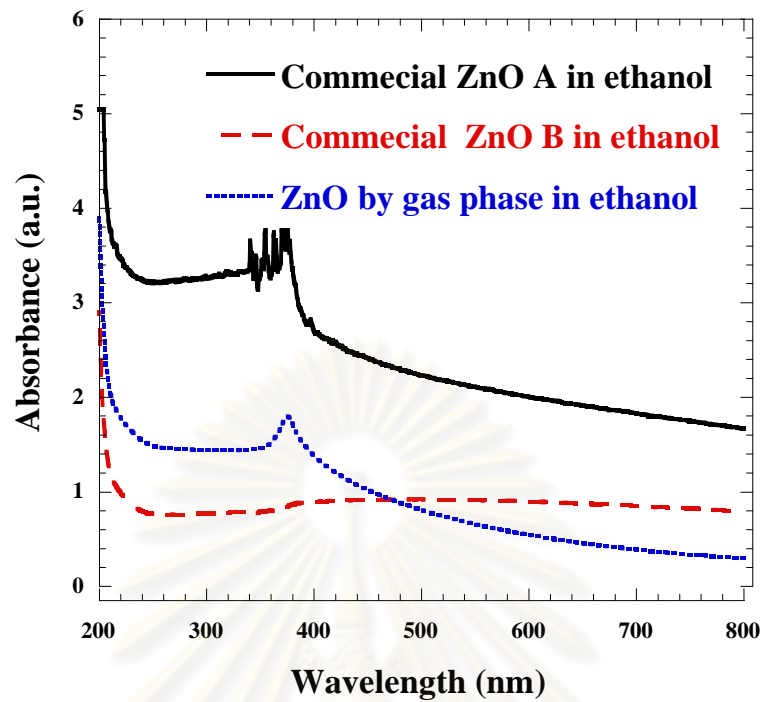
Figure 4.15 Effect of size and shape on absorbance of   ZnO in ethanol
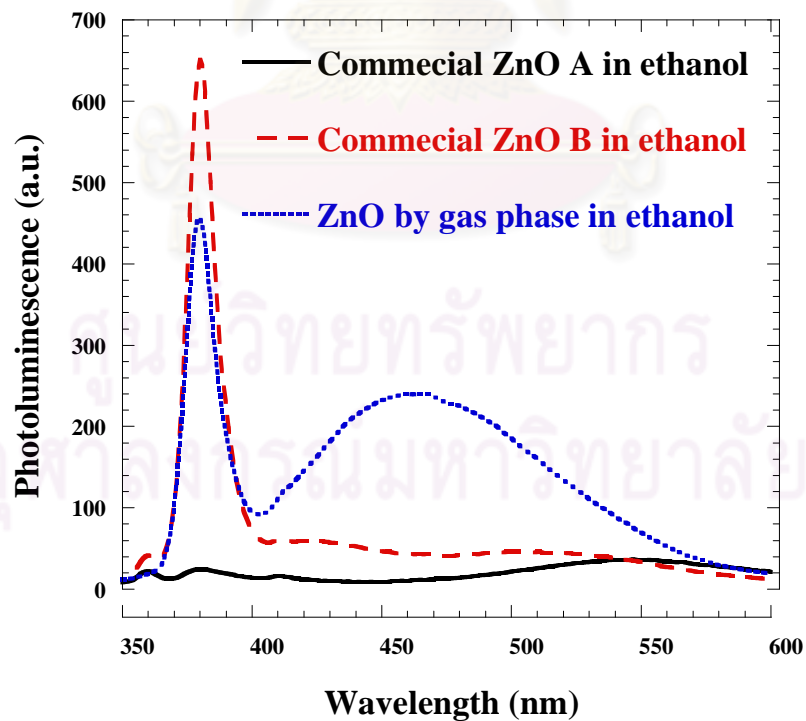
Figure 4.16 Effect of size and shape on the photoluminescence of ZnO in ethanol

4.3 Characterization of PMMA/ZnO composite

PMMA/ZnO composites were investigated optical and mechanical properties. The effect of morphology and increasing concentration from 0-5 wt% of ZnO in PMMA was investigated in this section.

4.3.1 Optical properties of PMMA/ZnO composite

The ZnO commercial A was mixed with PMMA to obtain film composite. The effect of ZnO concentration on absorbance of   PMMA/commercial ZnO A composite film was shown in figure 4.17. The absorption of all films showed peaks at 359 nm. The absorption intensity above 359 nm continually increased when ZnO concentration in PMMA increased which could be due to the opacity of film which was confirmed by the appearance of PMMA/ ZnO film composite in figure 4.23.

Figure 4.18 showed the effect of commercial ZnO A concentration on the light emission intensity and wavelength of composite films. The films were excited at 325 nm. The pure PMMA film has three main peaks at 381, 468 and 531nm which may be come from a chemical in PMMA product process. Adding more ZnO particles into the film caused the light emission intensity increased and slightly red shifted from 383 to 400 nm and a weak peak at 468 and 531 nm still occurred. The red shift of emission was affected from an increasing of the particle size. [23-24]

However the light emission of PMMA/commercial ZnO A showed very low intensity when compared with PMMA/commercial ZnO B and PMMA/ZnO synthesized by gas phase reaction. From figure 4.13, the commercial ZnO A can absorb UV more than commercial ZnO B and ZnO synthesized by gas phase reaction 1-2 times. At same excitation wavelength at 325 nm PMMA/commercial ZnO A had excitation energy lower than commercial ZnO B and ZnO synthesized by gas phase reaction. Moreover the emission intensity was decreased which could be due to the inner filter effect. Inner filter effect occurs because of high concentrations of absorbing molecules. The light excitation and light emission were absorbed so the intensity of light emission was decreased. [29]

The absorbance and photoluminescence of PMMA/commercial ZnO B were shown in figure 4.19 and 4.20 respectively. The absorption of all concentration showed peak at 385 nm. Increasing of ZnO concentration in PMMA caused turbidity in the films. The light

emission of all concentration film is at 385 nm and did not shift (~1-2 nm). The highest light emission intensity is at ZnO 1 wt % in PMMA. Then increase ZnO concentration decreases light emission intensity. It may be attributed to the aggregation of ZnO particles.

The ZnO synthesized by gas phase reaction was mixed with PMMA to make composite film. The effect of ZnO concentration on absorbance and photoluminescence were investigated. The absorbances of PMMA/ZnO synthesized by gas phase reaction were shown in figure 4.21. When increasing concentration of ZnO particle the absorbance increased and the films were become opaque. The composite film showed strong absorption peak at 369.5 nm as seen in figure 4.22. The light emission intensity in UV region increased when adding more ZnO concentration. PMMA/ ZnO synthesized by gas phase reaction showed highest intensity at 3 wt% where the light emission peak enhanced by 21 and 2 times when compared with ZnO commercial A and B respectively which is attributed to smaller crystallite sizes of ZnO (confirmed with XRD and particle size distribution graph data).
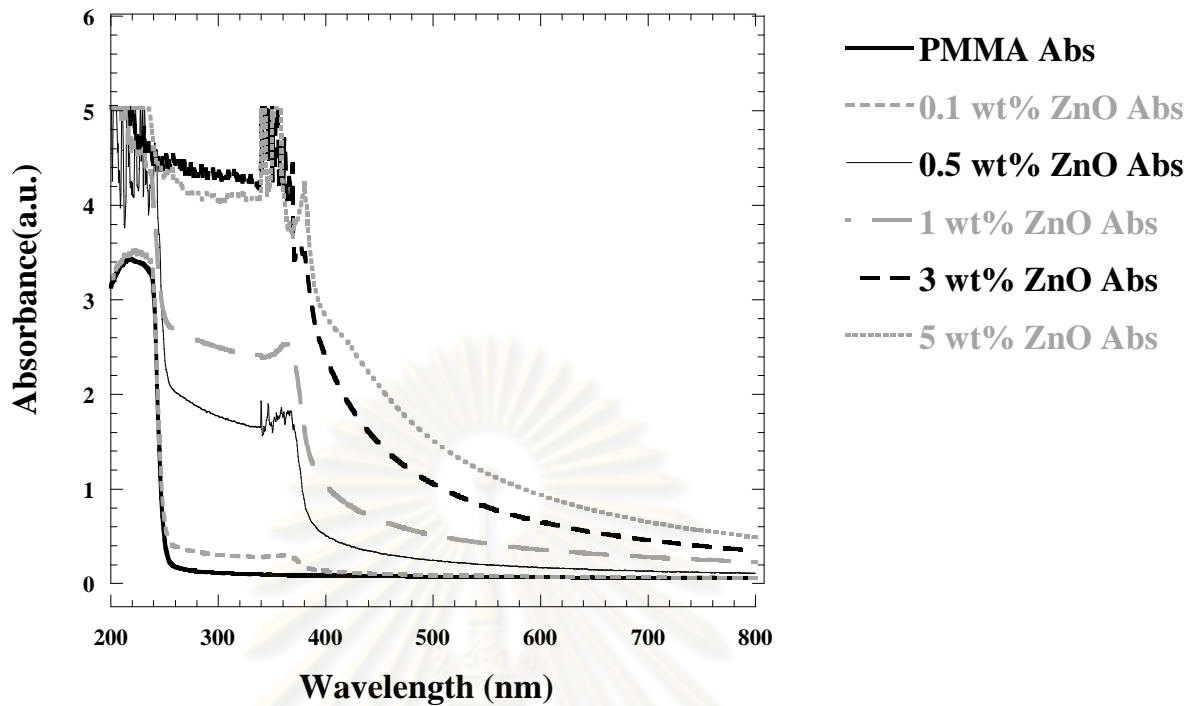
Figure 4.17 Effect of ZnO concentration on absorbance of
PMMA/Commercial ZnO A composite film
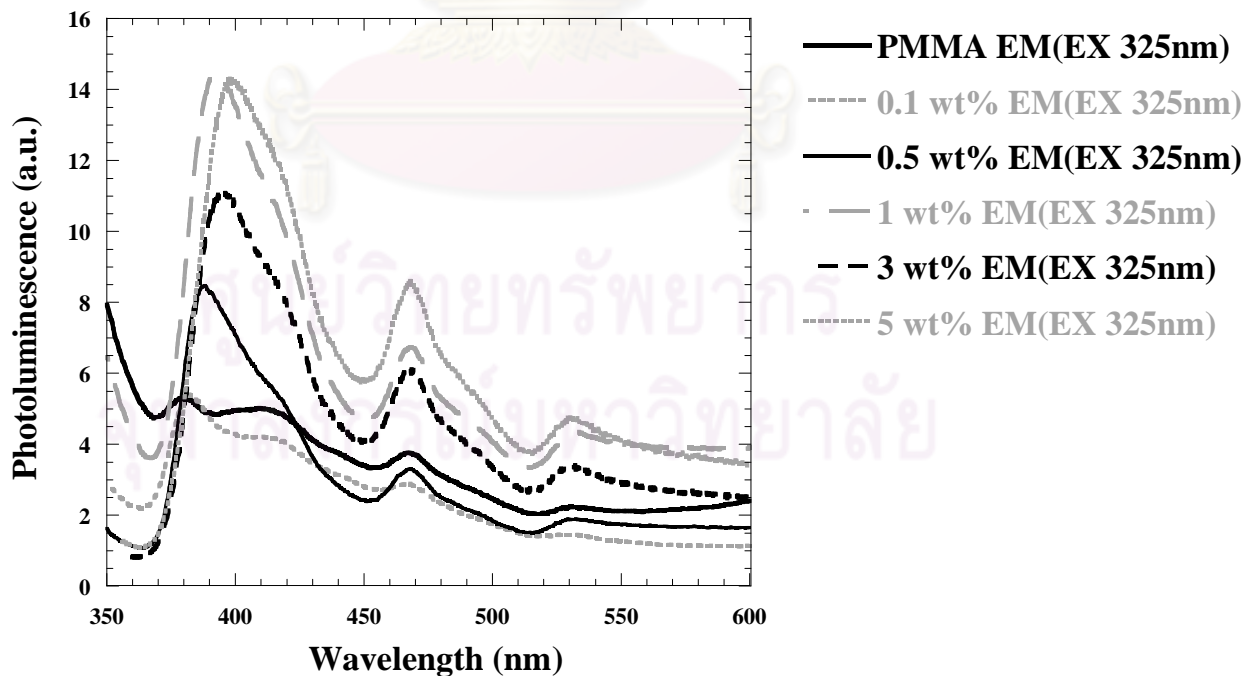
Figure 4.18 Effect of ZnO concentration on photoluminescence of
PMMA/Commercial ZnO A composite film
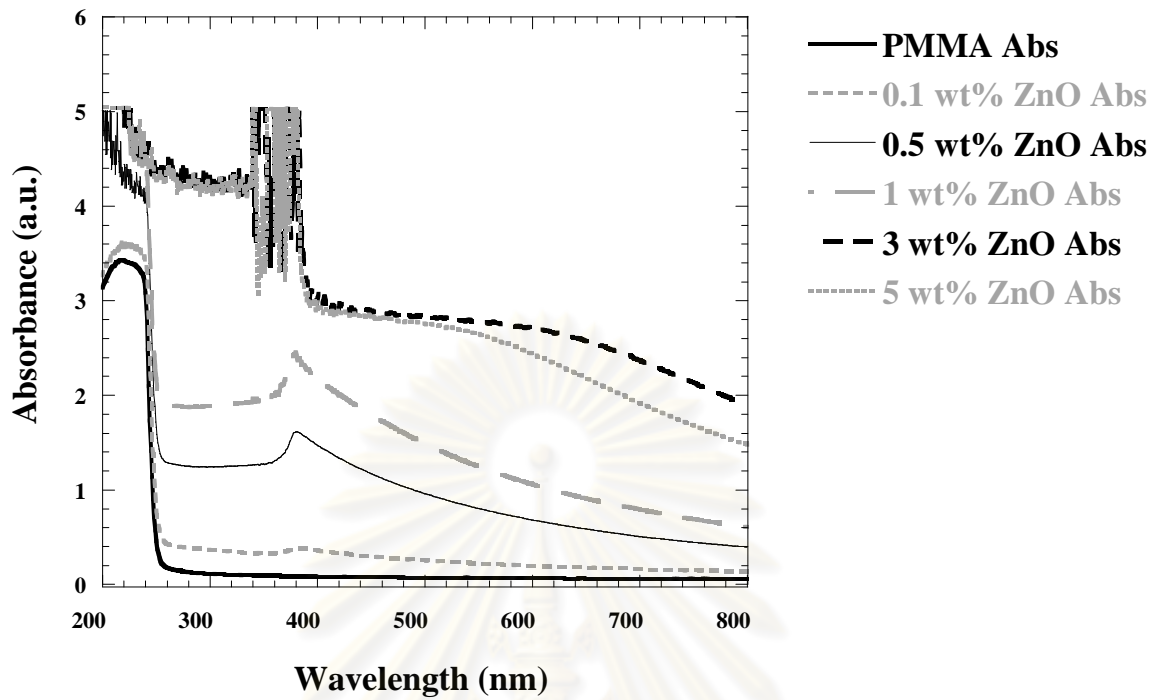
Figure 4.19 Effect of ZnO concentration on absorbance of

PMMA/Commercial ZnO B composite film
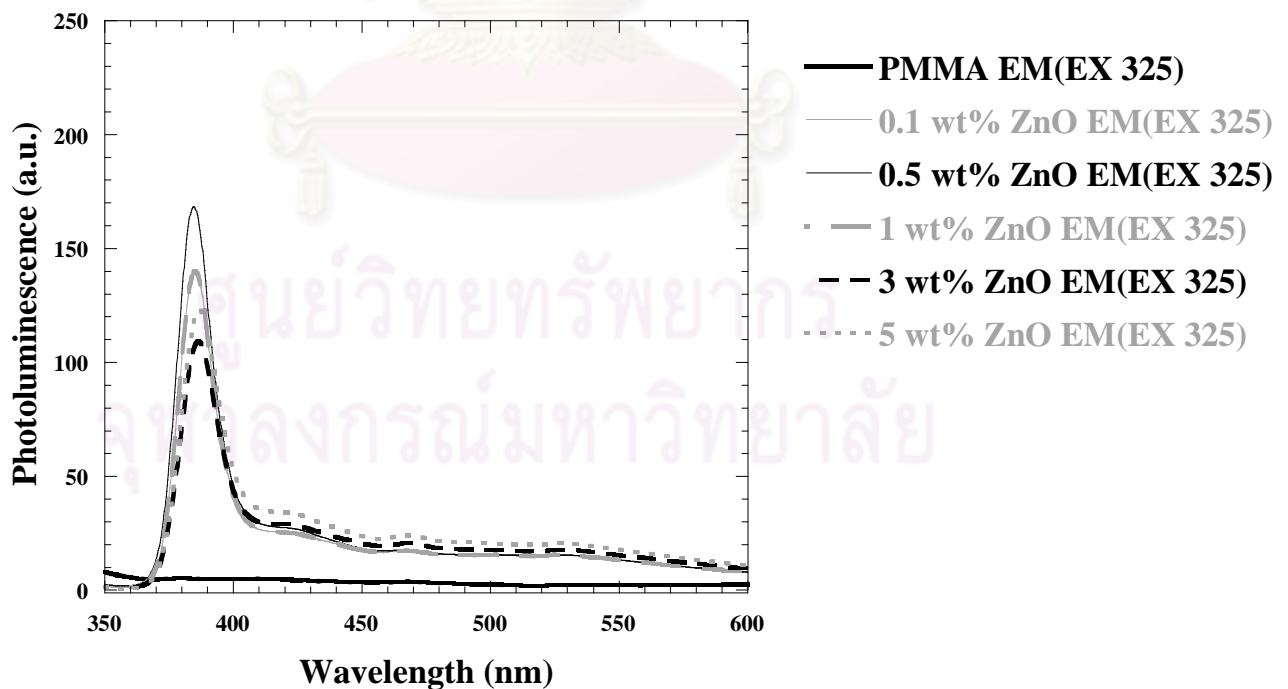
Figure 4.20 Effect of ZnO concentrations on photoluminescence of

PMMA/Commercial ZnO B composite film
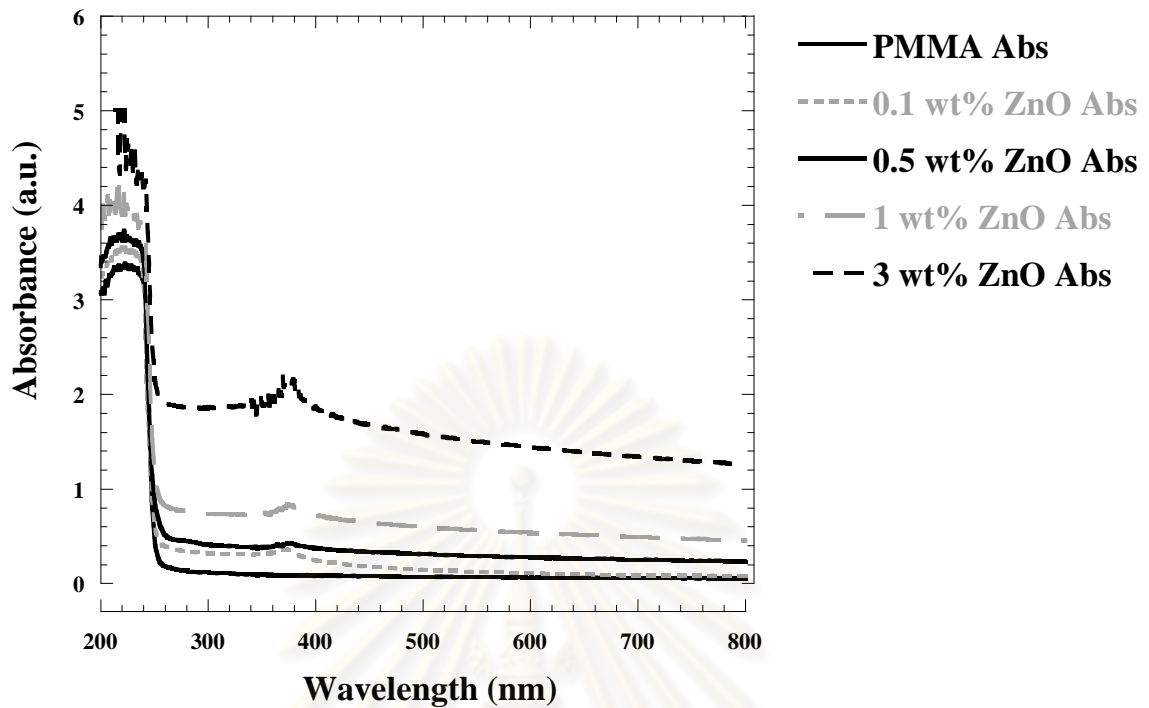
Figure 4.21 Effect of ZnO concentration on absorbance of PMMA/ZnO which
synthesized by gas phase reaction composite film
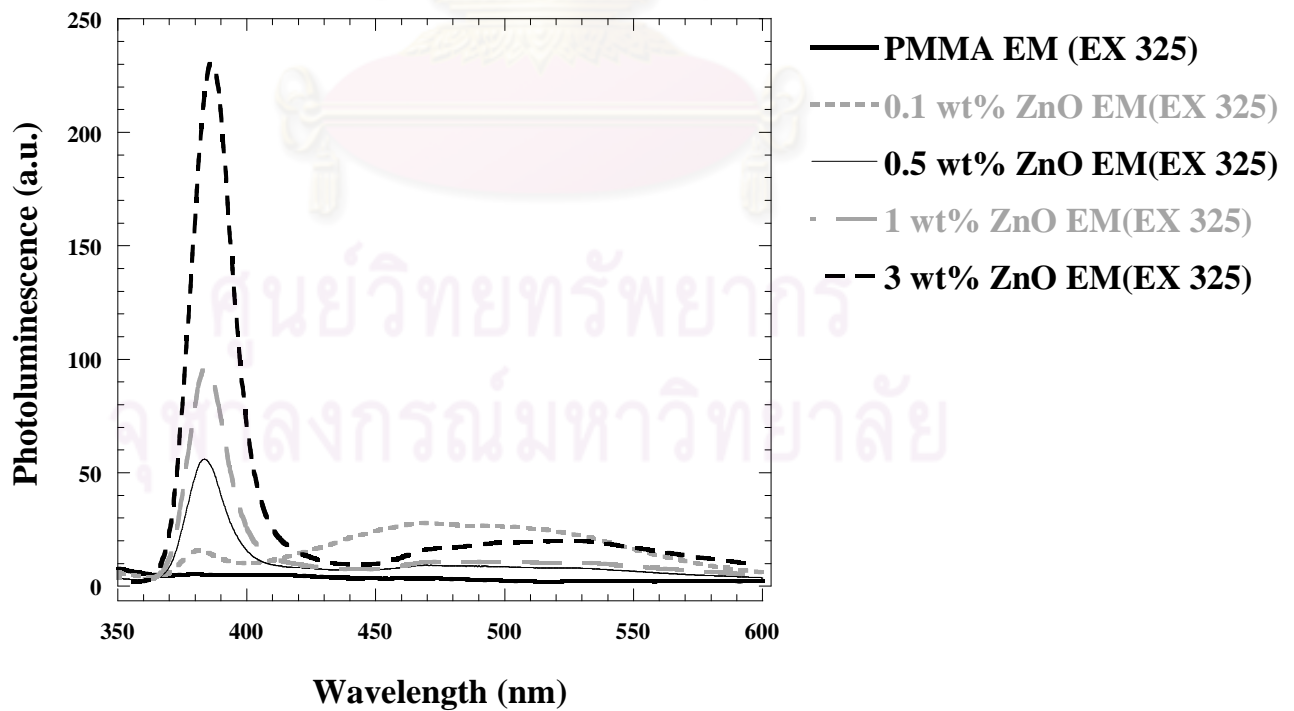
Figure 4.22 Effect of ZnO concentrations on photoluminescence of
PMMA/ZnO which synthesized by gas phase reaction

Figure 4.24a shows specific % transmittance of PMMA with commercial ZnO A composite film. Increasing of ZnO concentrations decreases the % transmittance. In case of PMMA with ZnO 5 wt%, it can shield UV and visible light because the film is opaque. On the other hand, the composite with 0.5 wt% of commercial ZnO A is good enough to shield UV rays. Xiong et al. also reported that 7 wt% of 60-nm ZnO particles completely shields UV ray for poly (stryrenebutylacrylate)/ZnO composite film, which is much higher compared to the concentration of ZnO commercial A particles [21]. Usually pure PMMA will have % transmittance nearly 100 %. However in this case Pure PMMA has % transmittance at 80% because on the composite film surface have small scratch. The % transmittance will be increase when decreasing the particle size.

The transmission of PMMA/ZnO commercial B composite film was shown in figure 4.24b. When the concentrations were increased more than 0.1wt% the UV light was shielded because commercial ZnO B particle showed highest UV absorption when compared with commercial ZnO A and ZnO synthesized by gas phase reaction. Moreover visible light were shielded due to the opacity of film.

The PMMA/ZnO synthesized by gas phase exhibited high transparency in UV and visible region. As ZnO synthesized by gas phase showed smaller size than ZnO commercial B and UV absorption properties was lowest when compared with commercial ZnO A and commercial ZnO B. Moreover PMMA/ZnO synthesized by gas phase showed highest luminescence intensity in UV range.

PMMA/commercial ZnO A showed higher transparency in visible light than PMMA/commercial ZnO B and PMMA/ZnO at the same concentration which was synthesized by gas phase reaction. Because the size of commercial ZnO A was smaller than commercial ZnO B and ZnO synthesized by gas phase reaction.
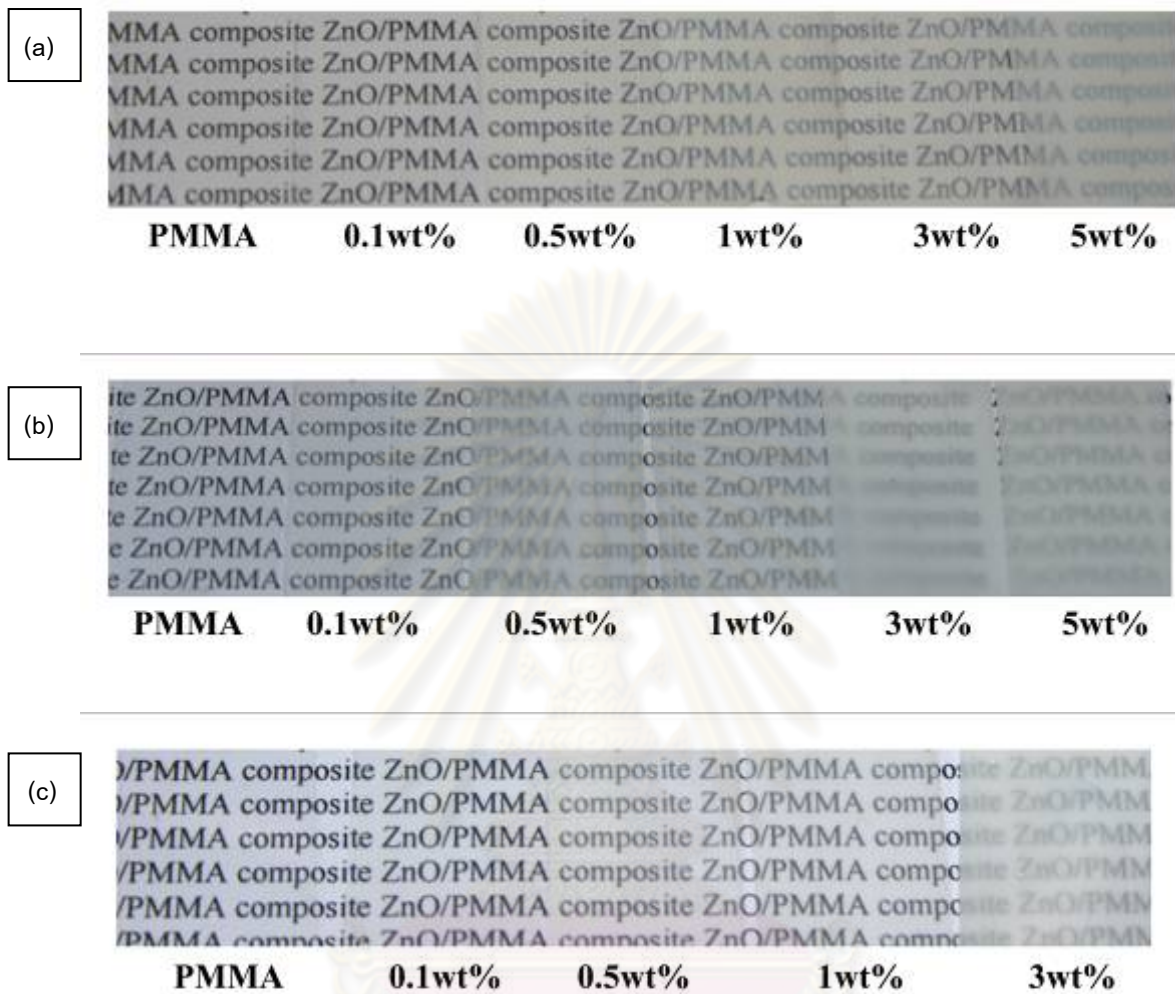
Figure 4.23 PMMA/ZnO when varying sizes and shapes of ZnO (a) PMMA with Commercial ZnO A, (b) PMMA with Commercial ZnO B and (c) PMMA with ZnO synthesized by gas phase reaction
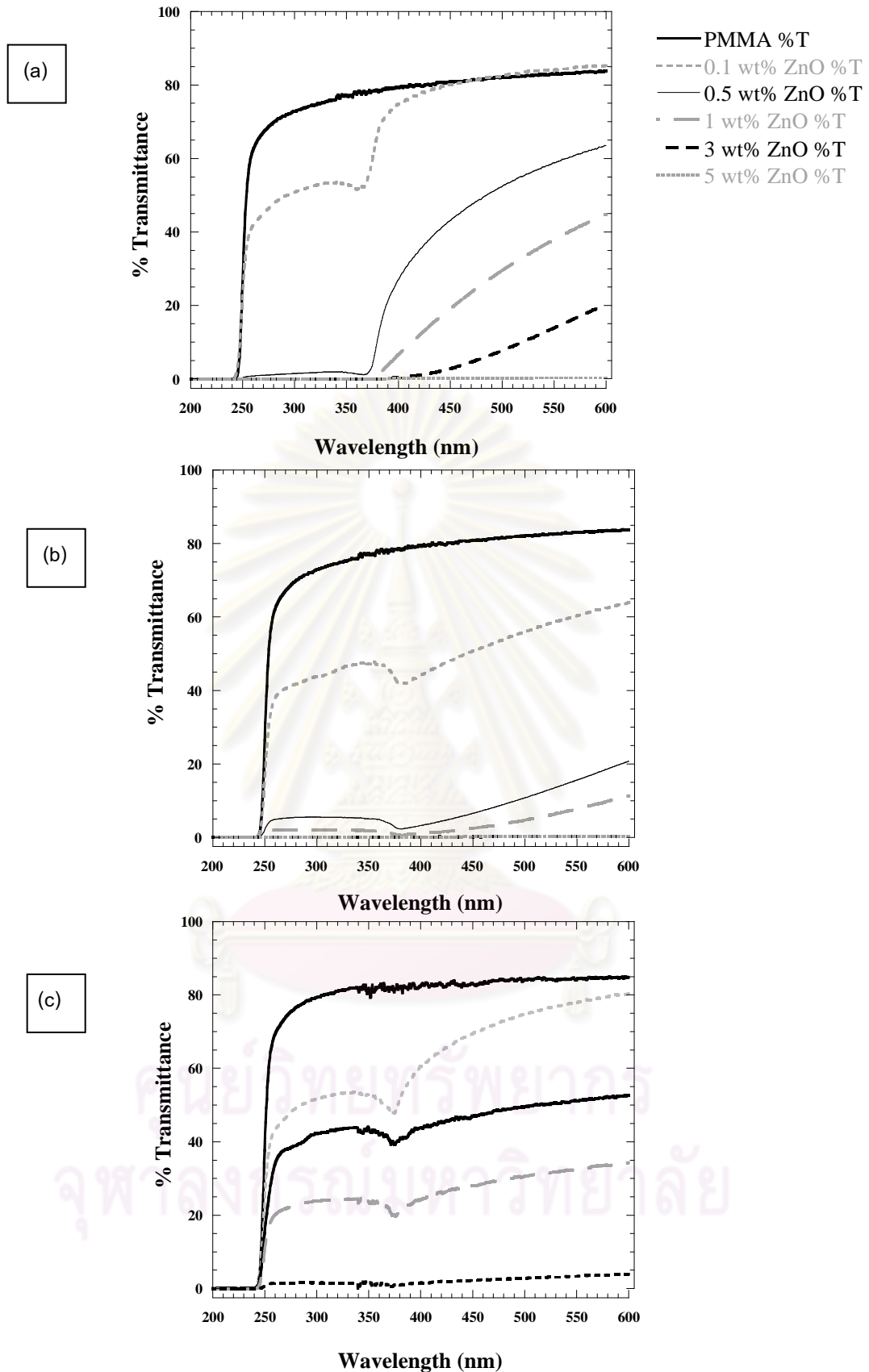
Figure 4.24 Transmission intensity of ZnO/PMMA composite when varying concentration of ZnO (a) Commercial ZnO A, (b) Commercial ZnO B and (c) ZnO synthesized by gas phase reaction

4.3.2   Thermal property of PMMA/ZnO composite

Glass transition temperature (T_g) of   PMMA/ZnO commercial A were characterized by dynamic mechanical analysis (DMA) under nitrogen atmosphere at heating rate 2°C/ min and frequency 10 Hz, temperature range from 60-150°C. The storage modulus is shown in figure 4.25. T_g of PMMA is 107 °C. T_g of PMMA/ ZnO 0.1, 0.5,1,3 and 5 wt% was quite the same at 107.0, 107.3, 107.4, 108.5 and 106.3 °C respectively when compared with that of pure PMMA. The results show that ZnO particle would not decrease the mobility of polymer chain.
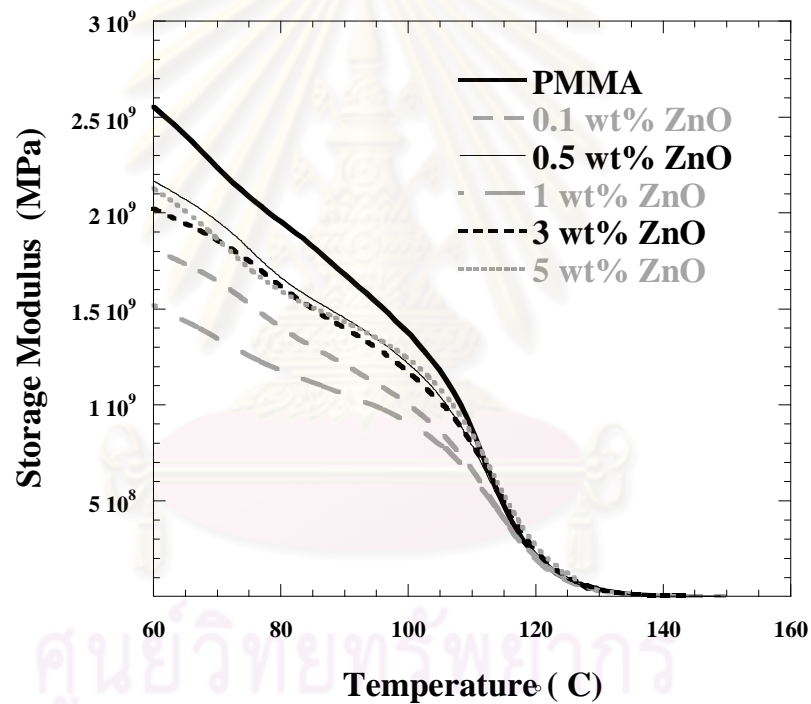
Figure 4.25 Storage modulus, E' of PMMA/Commercial ZnO A composite film

CHAPTER V

CONCLUSION AND RECOMMENDATION

5.1 Analysis of ZnO synthesis by gas phase reaction

The shape of ZnO particles which were deposited on quartz tube reactor depended on oxygen flow rate and collecting position in reactor. When oxygen flow rate was increased the morphology of synthesized ZnO changed from tetrapod to plate. The ZnO particles which were deposited on the rector wall at 100-400°C and at ambient temperature were bigger than ZnO which were deposited on the rector wall at 400-620°C. When particle collecting method was improved by making use of a particle filter the shape and size of collected ZnO particle was found to relate to the partial pressure oxygen inside the reactor. The partial pressure of oxygen was between 0.0132 and 0.034 atm ZnO nanoparticles were nearly sphere shape. While partial pressures of oxygen were between 0.034 and 0.056 atm, the particles which showed short leg were found.

5.2 Analysis of PMMA/ZnO composite

ZnO nanoparticles were dispersed in PMMA by using two-roll mill. PMMA/ZnO composite films prepared in this work could exhibit photoluminescence property. PMMA/commercial ZnO A composite film displayed the light emission range at 383-400 nm and showed red shifted compared to that of the pure PMMA films. Thereby, it is reasonable that the PMMA/commercial ZnO A composite film could shield UV irradiation in comparison with other composites using commercial ZnO B and ZnO synthesized by gas in-house. The 0.5 wt% of commercial ZnO A in PMMA could shield all UV and still show high transparency in visible light. Glass transition temperature of prepared PMMA/ZnO composite was at the same value as that of pure PMMA.

5.3 Recommendation for future work

In this work we propose that the partial pressure of oxygen is an important factor for growing leg of ZnO particle. But the synthesized size and shape of ZnO particle still non-uniform. Therefore we should investigate the effect of mixing between zinc vapor and oxygen by using mixing device.

The ZnO were synthesized by another condition should be made to obtain the composite to PMMA for investigate photoluminescence property. When concentration of ZnO was increased in polymer matrix the film became opaque. The opacity of film affected optical property. Then the surface of particle should be improved by some chemicals for more dispersion and protect the agglomeration of ZnO particle.

REFERENCES

[1] J. Zhang, Y.D.Yang, B.L. Xu, F.H. Jiang and J.P. Li. Shape-controlled synthesis
of ZnO nano- and micro- structures. Journal of Crystal Growth 280 (2005):
509-515.

[2] S. Mahamuni, B.S. Bendre, VJ. Leppert, C.A. Smith, D. Cooke, S.H. Risbud and
H.W.H. Lee. ZnO nanoparticles embedded in polymeric matrices.
NanoStructured Materials 6 (1996): 659-666

[3] C.H. Hung and W.T. Whang. Effect of surface stabilization of nanoparticles on
luminescent characteristics in ZnO/poly(hydroxyethyl methacrylate)
nanohybrid films. Journal of Materials Chemistry 15 (2005): 267-274

[4] Microtec lavoratory INC.Tichical Overview: Microncapsulation Technical Overview:
Microencapsulation[Online] Available from
http://www.microteklabs.com/technical_ovwrview.html

[5] J.H.Koo. Polymer Nanocomposite.McGraw-Hill,2006

[6] N. Pérez-Moral and A. G. Mayes, Comparative study of imprinted polymer
particles prepared by different polymerisation methods, Analytica Chimica
Acta 504 (2004):15-21

[7] K.D.Mielenz. Optical radiation measurements. New York: Acadimic press,1982

[8] J.E.Mark. Physical Properties of polymer Handbook. Second Edition, Springer,
2007

[9] U. Manzoo and, D.K. Kim, Size control of ZnO nanostructures formed in different
temperature zones by varying Ar flow rate with tunable optical properties
Physical E 41 (2009):500-505.

[10] S. J. Park, S. T. Lim, M. S. Cho, H. M. Kim, J. Joo and H. J. Choi. Electrical properties of multi-walled carbon nanotube/poly(methyl methacrylate) nanocomposite. Current Applied Physics 5 (2005):302-304

[11] J.F. Gong, H.B. Huang, Z.Q.Wang, X.N. Zhao, S.G. Yang and Z.Z. Yuc. A third kind growth model of tetrapod: Rod-based single crystal ZnO tetrapod nanostructure. Materials Chemistry and Physics 112 (2008): 749–752

[12] L. Shen, H. Zhang and S.Guo, Control on the morphologies of tetrapod ZnO nanocrystals. Materials Chemistry and Physics 114 (2008): 580-583

[13] S. Ren, Y.F. Bai, J. Chen, S.Z. Deng, N.S. Xu, Q.B. Wu and S. Yang. Catalyst-free synthesis of ZnO nanowire arrays on zice substrate by low temperature thermal oxidation. Materials letters 61 (2007): 666-670

[14] B.Y. Geng, X.W. Liu, X.W. Wei and S.W. Wang, Characterization and optical properties of regularly shape, single – crystalline sisal-like ZnO nanostructures. Materials letters 59 (2005): 3572-3376

[15] Z.G. Chen, A.Ni, F. Li, H.Cong, H.M.Cheng and G.Q. Lu. Synthesis and photoluminescence of tetrapod ZnO nanostructures. Chemical Physics Letters 434 (2007): 301-305

[16] C. Wu, X. Qiao, L. Luo and H. Li. Synthesis of ZnO flowers and their photoluminescence properties. Materials Research Bulletin 43 (2008): 1883–1891

[17] J. Lee, D. Bhattacharyya, A.J. Easteal and J.B. Metson. Properties of nano-ZnO/poly(vinyl alcohol)/poly(ethylene oxide) composite thin films. Current Applied Physics 8 (2008): 42–47

[18] C.H. Hung and W.T. Whang. Effect of surface stabilization of nanoparticle on luminescent characteristics in ZnO/poly(hydroxyethyl methacrylate) nanohybrid films. Journal of Materials Chemistry 15 (2006): 267-274

[19] E.J. Tang, G.X. Cheng and X.L. Ma. Preparation of nano-ZnO/PMMA composite particles via grafting of the copolymer onto the surface of zinc oxide nanoparticles. Powder Technology 161 (2006): 209 – 214

[20] Y.H. Hu, C.Y. Chen and C.C. Wang. Viscoelastic properties and thermal degradation kinetics of silica/PMMA nanocomposites. Polymer Degradation and Stability 3 (2004):545-553

[21] M. Xiong, G.Gu, B. You and L. Wu. Preparation and characterization of poly(styrene butylacrylate) latex/nano-ZnO nanocomposites. Journal of Applied Polymer Science 90 (2003): 1923 – 1931

[22] H. Liang, L. Pan and Z. Liu. Synthesis and photoluminescence properties of ZnO nanowires and nanorods by thermal oxidation of Zn precursors. Materials Letters 62 (2008): 1797-1800

[23] T. Kumpika, W. Thongsuwan and P. Singjai. Optical and electrical properties of ZnO nanoparticle thin films deposited on quartz by sparking process. Thin Solid Films 516 (2008): 5640–5644

[24] M. Wang, E K. Na, J. S. Kim, E. J. Kim, S.H. Hahn, C. Park and K.K. Koo. Photoluminescence of ZnO nanoparticles prepared by a low-temperature colloidal chemistry method. Materials Letters 61 (2007): 4094–4096

[25] M.Demir, M. Memes, P. Castignolles and G.Wegner. PMMA/Zinc Oxide Nanocomposites Prepared by In-Situ Bulk Polymerization. Macromolecular Rapid Communications 27 (2006): 763 – 770

[26] P.Nartpochananon. <u>Controlled synthesizes of ZnO nanoparticle using gas phase reaction</u>. Master's Thesis, Department of Chemical Engineering, Faculty of Engineering, Chulalongkorn University, 2008.

[27] Z Chen, N Wu, Z Shan, M Zhao, S Li, C.B. Jiang, M.K. Chyu and S.X. Mao. Effect of N_2 flow rate on morphology and structure of ZnO nanocrystals synthesized via vapor deposition. <u>Scripta Materialia</u> 52 (2005): 63-67

[28] Y.F. Hs, A.B. Djuris and K.H. Tam. Morphology and optical properties of ZnO nanostructures grown under zinc and oxygen-rich conditions. <u>Journal of Crystal Growth</u> 304 (2007): 47–52

[29] ลาวัลย์ ศรีพงษ์. <u>การวิเคราะห์เชิงฟลูออโรเมตรี</u>. นครปฐม: คณะเภสัชศาสตร์ มหาวิทยาลัย ศิลปากร, 2544

[30] A, Somwangthanaroj ,C. Phanthawonge, S. Ando andW. Tanthapanichakoon. Effect of the origin of ZnO nanoparticles dispersed in polyimide films on their photoluminescence and thermal stability. <u>Journal of Applied Polymer Science</u> 110 (2008): 1921 - 1928

APPENDICES

APPENDIX A

Temperature profile inside reactor

The temperature profiles of reactor (60 cm) were shown in figure A-1. The temperature in the reactor in which nitrogen flow rate was varied from 0 to 3 l/min was measured at 700 °C. The furnace position was at 10-40 cm. The nitrogen tube was at 5 cm. When nitrogen flow rate was increased the temperature profiles inside reactor were slightly changed.
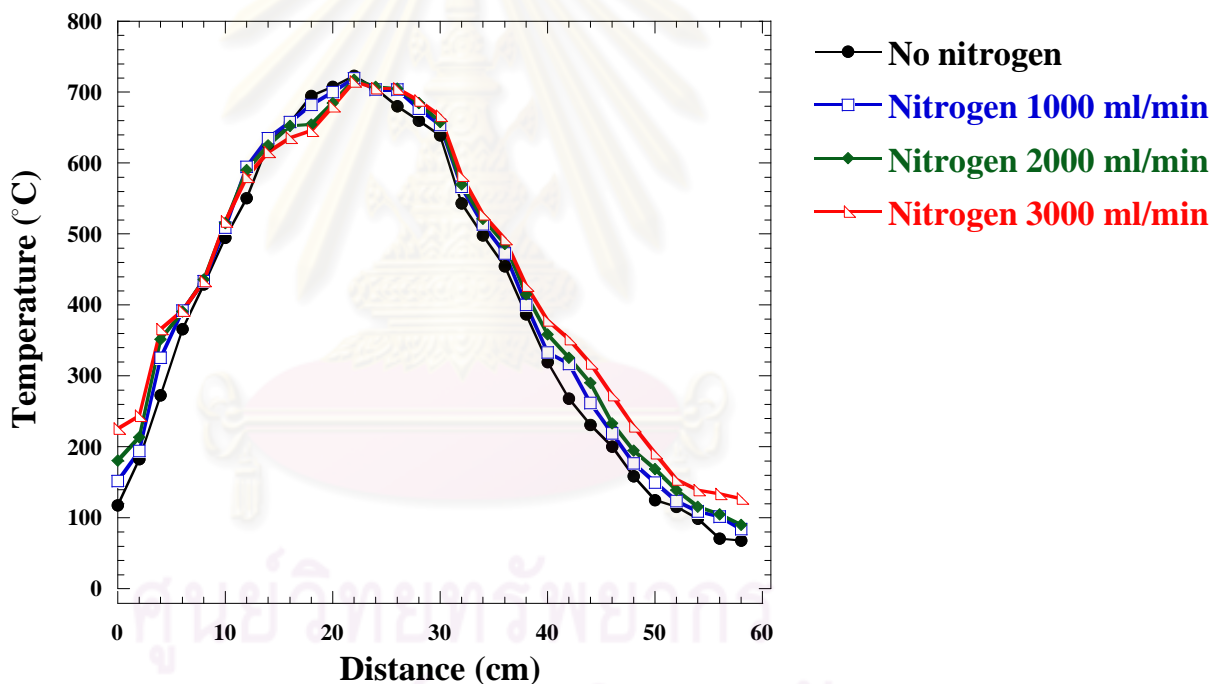
Figure A-1 Temperature profiles inside reactor (60cm)

The temperature profiles of reactor (120 cm) were shown in figure A-2. The temperature in the reactor in which nitrogen flow rate was varied from 0 to 3 l/min was measured at 600 °C. The furnace position was at 15-45 cm. The nitrogen tube was at 0 cm. When nitrogen flow rate was increased the temperature profile inside reactor were slightly changed.   At the 80 cm of reactor, the temperature profile decreased until reaching room temperature.
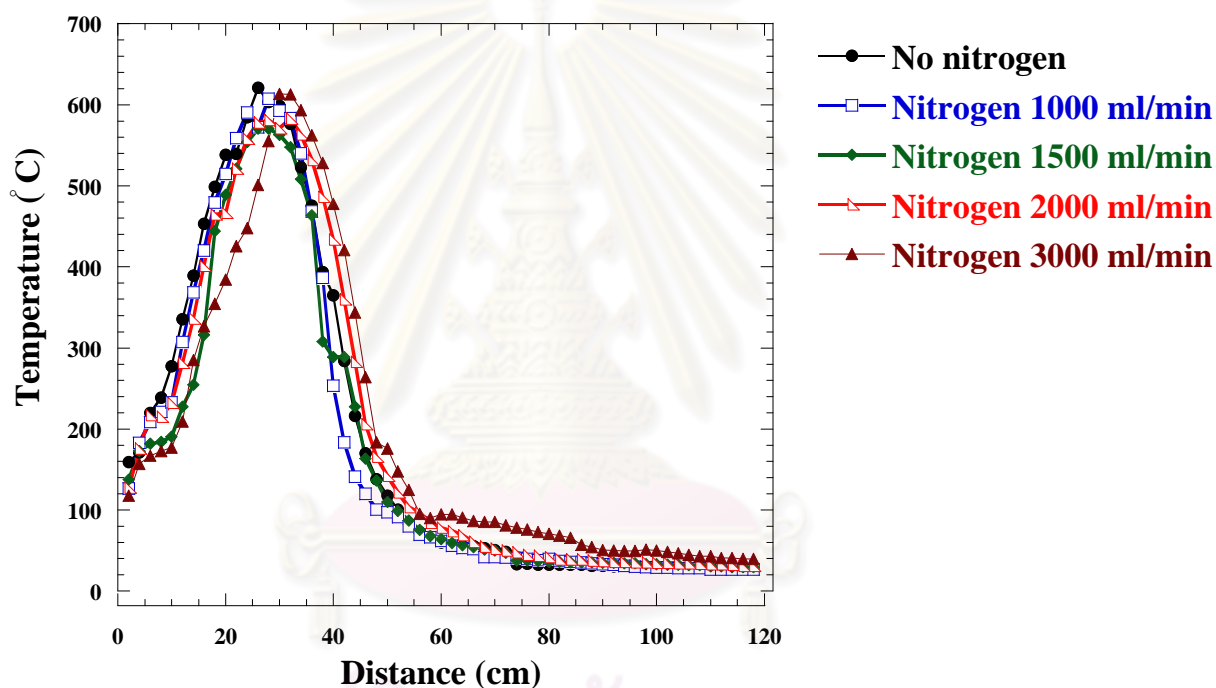
Figure A-2 Temperature profiles inside reactor (125cm)

APPENDIX B

Calculation of partial pressure

Partial pressure of zinc vapor and oxygen was calculated by using ideal gas mixtures. The mole fraction of an individual gas component in an ideal gas mixture can be expressed in terms of the component's partial pressure or the moles of the component:

$$x_A = n_A/n \qquad\qquad (A1)$$

$$p_A = x_A \times p \qquad\qquad (A2)$$

where :

n	=	total moles of the gas mixture
p_A	=	partial pressure of gas component A in gas mixture
n_A	=	moles of gas component A in gas mixture
x_A	=	moles fraction of gas component A in gas mixture
p	=	pressure of gas mixture

For example, in case of 20 ml/min of oxygen and 1000 ml/min of nitrogen flow rate

Mole of oxygen, nO_2
$$= \frac{0.02[l/\min] \times 1.429[g/l]}{32[g/mole]}$$
$$= 8.93 \times 10^{-3} \quad \text{mole/min}$$

Mole of nitrogen, $nN_2 = \frac{1[l/\min] \times 1.251[g/l]}{28[g/mole]}$
$$= 4.46 \times 10^{-2} \quad \text{mole/min}$$

Total mole
$$= 4.56 \times 10^{-2} \quad \text{mole/min}$$

Mole fraction of oxygen, $xO_2 = \dfrac{8.93 \times 10^{-3}}{4.56 \times 10^{-2}}$

$= 0.020$

We assume that partial pressure inside reactor is 1 atm. Therefore, partial pressure of gas component is equal to mole fraction.

APPENDIX C

The average size of the crystal

The average size of the crystal ZnO particles were calculated by Scherrers's formula equation as shown below.

$$D = \frac{0.9\lambda}{\beta \cos\theta}$$

Where D = average size of the ZnO crystallites

λ = the wavelength of the X-ray, 1.5418°A

β = line width at half maximum of peak

θ = Bragg angle of the diffraction peaks

Diffraction angle of crystal ZnO was measured by XRD. The value of 2θ peak is 36.2242° in which average size of ZnO crystal was calculated as follows.

$$D = \frac{(0.9 \times 1.5418)}{\left(0.0088 \times \dfrac{\cos 46.2242}{2}\right)}$$

$$D = 21.12°A$$

$$D = 2.112nm$$

APPENDICE D

International conference

Thornchaya Satitpitakun, Pat Natpochananon , Anongnat Somwangthanaroj, Yoshio Otani and Tawatchai Charinpanikul, Thermal srability of PMMA film composite with Zince oxide synthesized by gas phase reaction, Proceeding of Pure and Applied Chemistry International Conference (PACCON 2008), Bangkok Thailand,30 January 2008-1February 2008.

Thornchaya Satitpitakun, Pat Natpochananon , Anongnat Somwangthanaroj, Yoshio Otani, Koh-he Nitta and Tawatchai Charinpanikul, Application of ZnO nanoparticles for improving mechanical   and optical property of PMMA film, Proceeding of Japan association of aerosol science and technology (JAASC), Kanazawa Japan, 20-22 August 2008.

Thornchaya Satitpitakun, Hisashi Yamamoto, Anongnat Somwangthanaroj Yoshio Otani, Takafumi Seto, Koh-he Nitta and Tawatchai Charinpanikul, Dependence of UV abortion and mechanical characteristics of PMMA/ZnO composite on ZnO nanoparticle properties, Proceeding of Powder Technology Japan (Powtex 2008), Tokyo Japan, 30-31 October 2008,
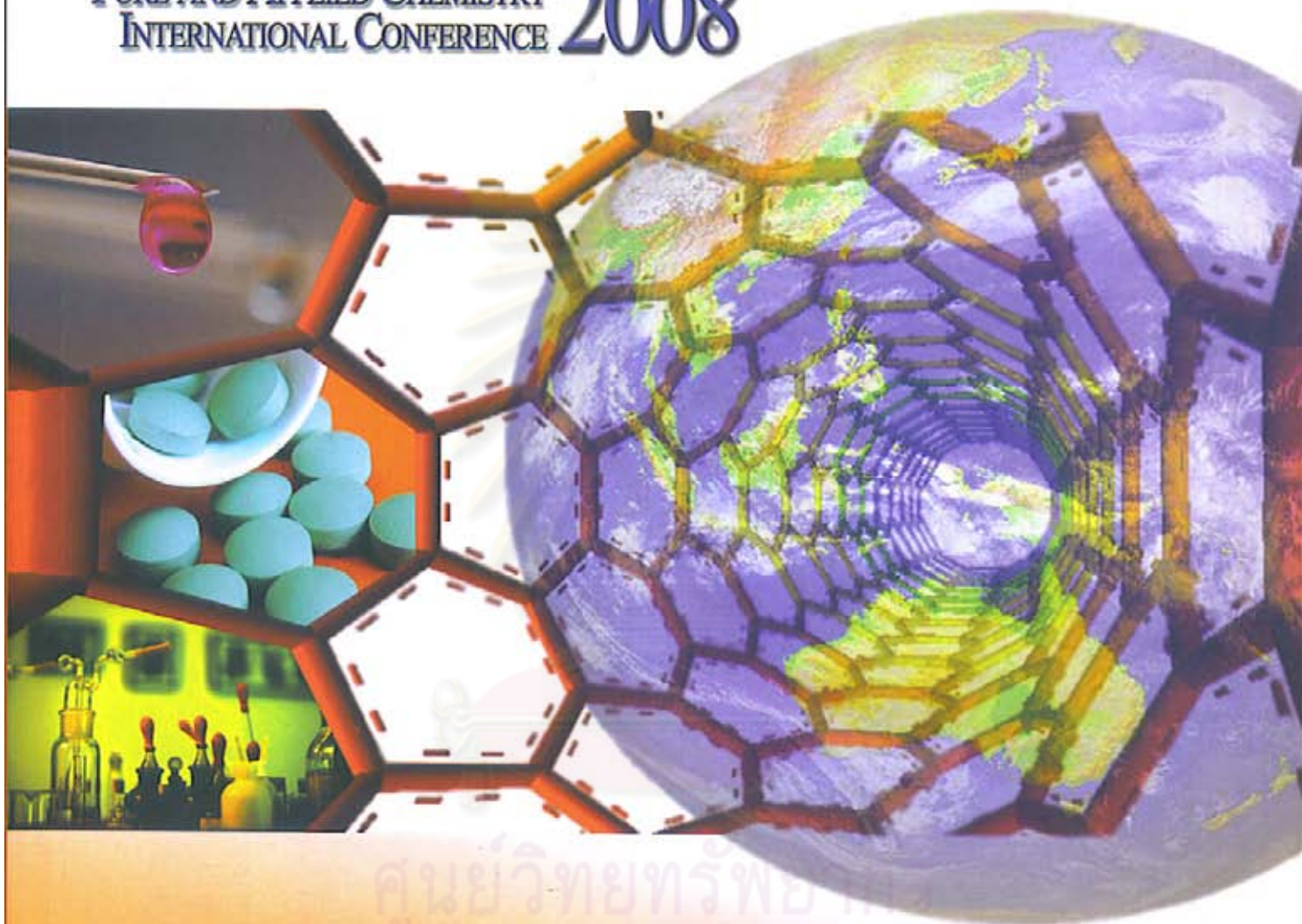
Thornchaya Satitpitakun, Hisashi Yamamoto, Anongnat Somwangthanaroj Yoshio Otani, Takafumi Seto, Koh-he Nitta and Tawatchai Charinpanikul, Improvement of thermo-mechanical and UV absorption of PMMA with ZnO nanoparticles, Proceeding of Thai student's association in Japan under Royal patronage(TJIA 2008), Tokyo Japan, 21 November 2008

S5-OR-20

Thermal Stability of Pmma Film Composited with Zinc Oxide Synthesized by Gas Phase Reaction

T. Satitpitakun[1], P. Natpochananon[1], A. Somwangthanaroj[2], Y. Otani[3], T. Charinpanikul[1]

[1]Center of Excellence in Particle Technology, Faculty of Engineering,
Chulalongkorn University, Patumwan, Bangkok
[2]Polymer Engineering Laboratory, Dept. of Chemical Engineering
Faculty of Engineering, Chulalongkorn University, Patumwan, Bangkok
[3]Dept of Chemical Engineering, Faculty of Engieering,Kanazawa University, Kanazawa
*E-mail: polar_pink@hotmail.com Tel: +66-2-218-6899

Tetrapod ZnO nanoparticles have been successfully synthesized by a gas phase reaction with oxygen flow control. Synthesized ZnO nanoparticles are mixed with polymethyl metacrylate (PMMA) for preparing nanocomposite film using bulk polymerization of methacrylic acid (MMA), in the presence of benzoyl peroxide (BPO). Effects of O_2 flow rate and temperature profile along the reactor on characteristics of ZnO nanoparticle characteristics, which are crystal structure, morphology and size have been investigated by X-ray diffraction (XRD), scanning electron microscopy (SEM) and transmission electron microscopy (TEM). An increase in N_2 flow rate results in formation of tetrapod ZnO nanoparticles with shorter pod length. Meanwhile, an increase in O_2 flow rate provides ZnO nanoparticle with plate-like morphology. At the O_2 flow rate of 20 sccm, the smallest tetrapod ZnO nanoparticles with a hexagonal wurtzite structure could be obtained. Then effect of tetrapod ZnO nanoparticle concentration on the thermal stability of the composite film has been investigated using TGA analysis.

ACKNOWLEDGEMENT

ศูนย์วิทยทรัพยากร
จุฬาลงกรณ์มหาวิทยาลัย

第 25 回

エアロゾル科学・技術研究討論会
国際シンポジウム 2008
講演要旨集

Abstract of the 25th Symposium on
Aerosol Science & Technology
in conjunction with
International Aerosol Symposium 2008

August 20～22, 2008

Kanazawa, Japan

日本エアロゾル学会

Japan Association of Aerosol Science and Technology

P 02

Application of ZnO nanoparticles for improving mechanical and optical property of PMMA film

T.Satitpitakun[1], P. Natpochananon[1], A. Somwangthanaroj[1], Y. Otani[2], K. Nitta[2] and T. Charinpanikul[1]
[1]Center of Excellence in Particle Technology,
Department of Chemical Engineering. CHULALONGKORN University, THAILAND
[2] Department of Chemical Engineering.
Graduate School of Natural Science and Technology, Kanazawa University, JAPAN

Abstract

In this present work, ZnO nanocomposites. 20nm, with 0-5 wt% concentration of polymethyl metacrylate (PMMA) were prepared by melt extrusion. The optical property and dynamic mechanical properties of ZnO and PMMA have been investigated. Polymer as a surface capping agent for nanoparticles is commonly because it could easily be fabricated in various forms including thin film. Many researchers have actively focused on the superior emitting properties of the nanocomposite of nanoparticles and a polymeric matrix. Consequently, ZnO/PMMA composites were successfully prepared by two roll mixing. The concentration of ZnO nanoparticles in PMMA has been varied for examining its effect on the properties of ZnO/PMMA composite by Dynamic Mechanical Analyzer, ultraviolet–visible (UV–vis) spectrophotometer

Introduction

Zinc Oxide (ZnO) is a semiconducting oxide with a wide band gap of 3.4 eV and a large exciton binding energy of 60 meV [1]. The various nanostructures of ZnO including nanowires, nanotubes, nanobelts and nanoneedle have been synthesized and investigated by variety of techniques chemical such as vapor deposition, pyrolysis, hydrothermal method and so on [2]. ZnO nanoparticles, as one of the multifunction inorganic, have drawn increasing attention in recent year due to its many significant physical and chemical properties, such as chemical stability, ultraviolet and infrared adsorption[3]. Poly(methyl methacrylare) (PMMA) is an optically clear thermoplastic. It is widely as a substitute for inorganic glass, because it show higher impact strength, resistant to weak acids, alkaline solutions, non-polar solvents, oils and water. It is new well established that the polymers are excellent host materials for nanoparticles of metal and semiconductors. When the nanoparticles are mixed with polymer, the polymer will act as surface capping agent because the polymer can be built to be a film easily and the particles is controlled well within many conditions. Many research groups have focused on the superior emitting properties of nanocomposites by dispersing the particles into a polymeric matrix. The hybrid nanocomposites not only inherit the high luminescence but also possess advantages of polymers such as flexibility, film integrity and thermal stability [4-5].The concentration of ZnO nanoparticles in PMMA has been varied. The mechanism property of ZnO/PMMA composite was investigated

Experimental

Preparation of ZnO/PMMA composites

ZnO 0.02μm from Wako Pure Chemical Industries, Ltd. and PMMA from Negami Chemical Industrial Co., Ltd. The concentrations of ZnO nanoparticles were varied (0, 0.5 l, 3 and 5 wt%). The composite were mixed on two roll mill at 200°C for 10 minute. The mixed were compression molded into 0.05 mm thick sheets by using a hot plated, hydraulic, compression molding machine. The temperature of hot plates was 200°C and 100 kft/cm² pressures were applied on molds. After 5 min the molds were cooled to ambient temperature using water at 0°C

Characterization

The optical properties were studied by UV–Vis-NIR spectrometry (Jasco V570). The scan speed was 400 nm/min in the range of 200-800 nm wavelengths.

A dynamic mechanical analysis of the composites was performed using a DVE-V4 FT Rheospectrer. Dynamic Mechanical Analyzer at a heating rate of 1 °C/min and frequency 10 Hz. Sample dimensions were typically 20 mm long, 5 mm wide, and 0.20 mm thick.

Results and Discussion

UV abortions

ZnO 20 nm were make to be composite with PMMA. Fig 1 show the absorption peak appears at 365-380 nm from the nanocomposite. The wavelength shifted when increase concentration of ZnO. Chin et al study effect of surface stabilization of nanoparticles on luminescent characteristics in ZnO / poly (hydroxyethyl methacrylate) nanohybrid . When ZnO agglomerates to be bigger the peak of UV absorbance peak will shift.[6] The intensity of UV absorbance peak increases with increment of ZnO/PMMA composite. This optical change results from a quantum effect of the nanoparticles when the size of particles is reduced to a nanoscale [7]. Therefore, the nanocomposite prepared in this study can protect against UV light. This means that nano-ZnO/PMMA composites can improve the weather ability of the coatings film.
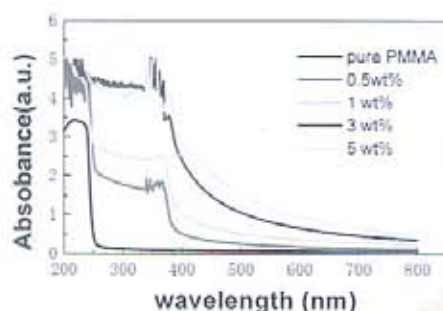
Fig 1 UV-Abortions spectra of ZnO/PMMA

Fig 3. Loss modulus, E'', of the ZnO/PMMA nanocomposites with various ZnO contents

Viscoelastic properties of modified ZnOPMMA Nanocomposites

The storage modulus (E'') and tan δ properties of the composites were characterized by Dynamic mechanical analysis (DMA). The storage modulus connects with the elastic modulus of the materials, and the loss modulus relates to the energy lost duto polymer chain movement. Fig 2 the storage modulus composite (E'') for the composites containing lower amount ZnO (0.5 wt%) is higher than that of pure PMMA in given range 50 to 275 °C. The stiffness associated with the modified ZnO particles dispersed well within the PMMA matrix causes the storage modulus to increase with ZnO content. Fig. 3 indicates that T_g of the ZnO/PMMA nanocomposites increased with the ZnO content. The T_g of these ZnO/PMMA composites exceeds that of pure PMMA because the well-dispersed ZnO layers restrict the mobility of the PMMA chain and the ZnO surface is entangled with the PMMA molecule Fig 4 plots the dependence of tan δ on temperature for ZnO/PMMA nanocomposites. The loss factor tan d is very sensitive to the structural transformation of the materials. Adding ZnO particles to the PMMA matrix shifts the tan δ peak values of composites to the high temperature region, implying an interaction between ZnO and the PMMA molecules.

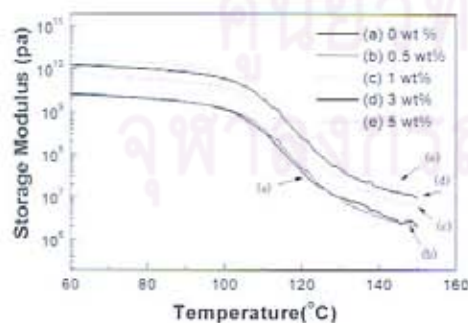Fig 4. tanδ of ZnO/PMMA nanocomposites with various ZnO contents

Conclusions

ZnO/PMMA nanocomposite are synthesized by two roll mill. When concentration of ZnO increase-abortions increase. The result indicates that the ZnO/PMMA nanocomposite films with higher ZnO content exhibits higher glass transition temperature and storage modulus than pure PMMA.

References

[1] Zhao, J.W.; Qin, L.R.; Xiao,Z.D.; Zhang,L.D. Materials Chemistry and Physics 2007,105,194-198
[2] Hu, H.; Huang, X.; Deng, C.; Chen. X.; Qian, Y. Materials Chemistry and Physics 2007,106, 58–62
[3] M.M. Hana.; S.M. Eltaib.; M.B. Ahmad. European Polymer Journal 2000, 36, 2081-2088
[4] W, Z.G.; Zu,X.T.; Zhu,S.; Xiang, A.; Fang,L.M.; Wang,L.M. Physics Letters A:2006,350,252-257.
[5] Singh, N.; Khanna, P.K. Materials Chemistry and Physics 2007,104,367-372.
[6] R M. Nyffenegger.; B.Craft.; M Shaaban.; S.Gorer.; G. Erley.; R M. Penner.; Chem. Mater. 1998, 10, 1120-1129

Fig 2. Storage modulus, E', of the ZnO/PMMA nanocomposites with various ZnO contents

2008年度
秋期研究発表会講演論文集

日　時　　2008年10月30日（木）
　　　　　　10月31日（金）

会　場　　幕張メッセ国際会議場
　　　　　　（千葉市美浜区中瀬2-1）

粉 体 工 学 会

S1-5

Dependence of UV abortion and mechanical characteristics of PMMA/ZnO composite on ZnO nanoparticle properties

T.Satitpitakun[1], H. Yamamoto[2], A. Somwangthanaroj[1], Y. Otani[2],
T.Seto[2], K. Nitta[2] and T. Charinpanikul[1]
[1]Center of Excellence in Particle Technology,
Department of Chemical Engineering, CHULALONGKORN University, THAILAND
[2] Department of Chemical Engineering, Graduate School of Natural Science and Technology,
Kanazawa University, JAPAN, TEL:+81-76-234-4813, e-mail:otani@t.kanazawa-u.ac.jp

Poly(methylmetacrylate)/ZnO nanocomposite was fabricated by a melt mixing method. PMMA was kneaded using a two-roll mill and mixed with ZnO particles with various sizes and concentrations in order to investigate the effect on the optical and mechanical properties of the composite film. As a result, ZnO nanoparticles were uniformly dispersed in PMMA polymer by using the two-roll mill. ZnO nanoparticles in nanocomposite film effectively shielded UV rays compared to micrometer-size ZnO particles. Furthermore, ZnO nanoparticles shifted the glass transition temperature of PMMA to a higher temperature with an increase in ZnO concentration.

1. Introduction

Composite materials between metal oxide and polymer have been investigated in order to improve their matrix properties. Nanoparticles /polymer matrices have attracted interest because of the unique mechanical, great optical properties. The mechanical and thermal properties of inorganic/organic nanocomposite are expected to be considerably improved when the largest inorganic surface area is present in the matrix [1]. ZnO is an important compound semiconductor material because of its wide band gap (3.3 eV), high excitation binding energy (60 meV) at room temperature [2]. Poly (methyl methacrylare) (PMMA) is an optically clear thermoplastic materials. It is widely used as an artificial glass, because it shows higher impact strength, resistant to weak acid or alkaline solutions, non-polar solvents, oils and water. The objective of present work is to improve optical and mechanical properties of PMMA film with ZnO nanoparticles. The effects of size and concentration of ZnO particles on UV abortion and dynamic mechanical properties were studied.

2. Experimental

ZnO powders with the nominal average particle sizes of 20 nm and 5 μm were purchased from Wako Pure Chemical Industries. PMMA was obtained from Kuraray Co.,LTD Fig.1 shows typical SEM image of ZnO with nanometer size. There are large ZnO particles with many small particles, resulting in the number-based average size of about 20 nm.

The PMMA and ZnO particles were mixed for 10 min at 200°C using a two-roll mill. The mixed materials were subject to a compression molding to prepare 0.5 mm thick films. The operating condition of the compression molding machine was 200 °C and 100 MPa. Then the specimen was immersed in 0°C water to cool it down.

The morphology of the ZnO nanoparticles obtained from each experiment was analyzed using scanning electron microscope (SEM Hitachi S4500). The optical properties of prepared specimens were studied by UV spectrophotometer (Jasco, V570). The scanning speed was 400 nm/min in the range of 200-800 nm wavelengths. The nanocomposite film samples were directly cut into rectangular shapes of 20mm×5mm×0.20mm. Dynamic mechanical analysis of the specimens was performed using a DMA (DVE-V4 FT) with a heating rate of 1 °C/min and frequency of 10 Hz.

3. Results and Discussion

ZnO particles with the nominal diameter of 20nm were added into PMMA at varies concentrations. Figure 2(a) shows the absorption curves at ZnO concentrations of 0.5, 1, 3 and 5 wt%. The intensity of UV absorbance peak increases with ZnO concentration.

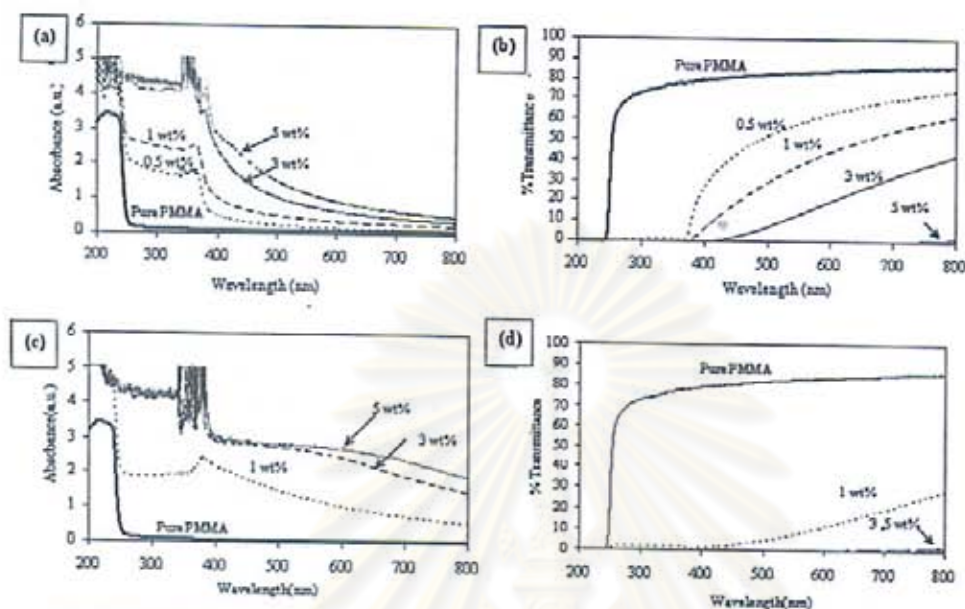Fig 1. SEM images of 20 nm ZnO particles.

Fig 2 Absorbance and transmittance of PMMA/ZnO: (a),(b) 20-nm ZnO and (c),(d) 5-μm ZnO

Although there are some noises in the absorbance curves at a high ZnO concentration, the peak absorption exists at the wavelength of 367 nm, which is smaller than 378 nm (the theoretical wavelength of bulk ZnO corresponding to band-gap of 3.3 eV). Whereas, in Fig.2 (c), the absorption peak exists at 378 nm for the polymer embedded with 5-μm ZnO particles. The blue-shift phenomenon for 20-nm ZnO particles is attributed to the quantum effect of nanoparticles. Fig.2 (b) shows specific absorption of UV light. In particular, the composite with 0.5 wt% of 20-nm ZnO is enough to shield UV rays. Xiong et al. also reported that 7 wt% of 60-nm ZnO particles completely shields UV ray for poly (stryrenebutylacrylate)/ZnO composite film, which is much higher compared to the concentration of 20-nm ZnO particles [3]. However as could be seen in Fig.2 (d), 5-μm ZnO particles exhibit insignificant UV absorption when compared with that of ZnO nanopartcles.
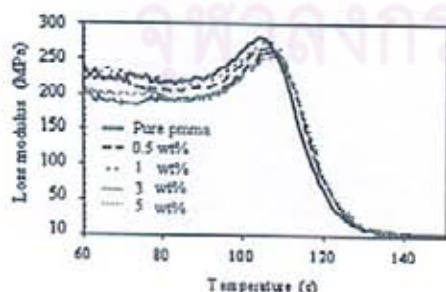

Fig.3 shows the loss modulus, E'', of 20-nm ZnO/PMMA composite film with various ZnO concentrations

Fig.3 shows the loss modulus, E'', of 20-nm ZnO/PMMA composite film with various ZnO concentrations. It is seen from Fig.3 that the glass transition temperature, T_g, shifts to a higher temperature with an increase in ZnO concentration. This may be attributed to the mobility restriction of PMMA chain due to the entangling ZnO particles within PMMA matrix. Xiong et al. reported that further increase in ZnO concentration leads to an decrease in T_g because of agglomeration of ZnO particles at a high ZnO concentration [3]. Since we do not observe any decrease in T_g with an increase in ZnO concentration, ZnO particles are uniformly dispersed in PMMA without agglomeration even at a high ZnO concentration with our mixing method.

4. Conclusions

ZnO nanoparticles are uniformly dispersed in PMMA polymer by using two-roll mill. ZnO nanoparticles in nanocomposite film effectively shields UV irradiation compared to micrometer-size ZnO particles. Furthermore, ZnO nanoparticles shift the glass transition temperature of PMMA to a higher temperature with an increase in ZnO concentration.

5. References

[1] Y.H. Hu, C.Y. Chen, C.C. Wang, Polymer Degradation and Stability. 84 (2004) 545-553
[2] P. Yang, H. Yan, S. Mao, R. Russo, J. Johnson, R. Saykally, N. Morris, J. Pham, R. He and H.-J. Choi, Adv. Functional Maters. 12(2002) 323 – 331.
[3] M.Xiong, G. Gu, B.You, L. Wu, Journal of applied polymer science. 90 (2003) 1923-1931
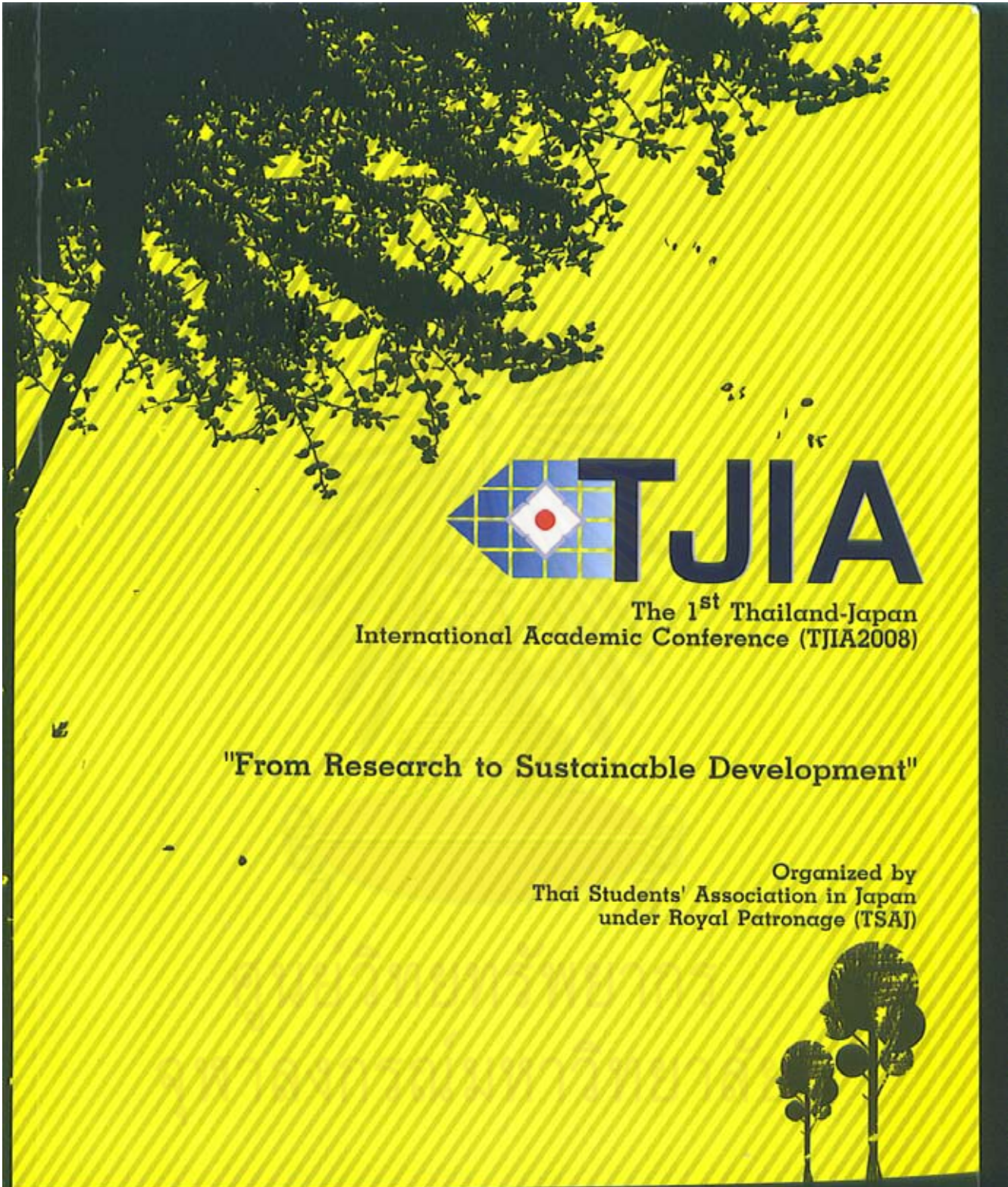
TJIA

The 1ˢᵗ Thailand-Japan
International Academic Conference (TJIA2008)

"From Research to Sustainable Development"

Organized by
Thai Students' Association in Japan
under Royal Patronage (TSAJ)

Presented by

Improvement of Thermo-mechanical and UV Absorption of PMMA with ZnO Nanoparticles

Thornchaya Satitpitakun[1], Hisashi Yamamoto[2], Anongnat Somwangthanaroj[1], Takafumi Seto[2], Yoshio Otani[2], Koh-hei Nitta[2], Tawachai Charinpanikul[1,*]

[1]Center of Excellence in Particle Technology,
Department of Chemical Engineering, Chulalongkorn University, Bangkok, Thailand
[2]Department of Chemical Engineering,
Graduate School of Natural Science and Technology, Kanazawa University, Japan
*Email address: ctawat@chula.ac.th

In this present work, poly (methyl metacrylate)/ZnO nanocomposite has been successfully fabricated by melt mixing method. The concentration of ZnO nanoparticles in PMMA has been varied for examining its effect on the properties of PMMA/ZnO composite by dynamic mechanical analysis (DMA) and ultraviolet–visible (UV–vis) spectrophotometry. The results indicated that the thermal stability of the prepared PMMA/ZnO composite could be significantly improved. The composite glass transition temperature shifted to a higher temperature with the increasing ZnO loading. Furthermore, UV absorption of ZnO PMMA composite was higher when ZnO concentration was increased and the composite with 0.5 wt% of 20-nm ZnO was sufficient for shielding UV irradiation.

1. Introduction

Because of the wide band gap (3.37 eV), high exciton binding energy (60 meV) at room temperature and high mechanical and thermal stabilities, zinc oxide (ZnO) is used as not only semiconductor but also functional filler for polymer composites [1]. Poly (methyl methacrylate) (PMMA) is an optically clear thermoplastic material. It is widely used as an artificial glass because it shows higher impact strength as well as resistant to weak acid, alkaline solutions, non-polar solvents, oils and water. Therefore, PMMA is commonly used for alternative constructing interior instead of glass. It is well recognized that PMMA is excellent host material for nanoparticles of metal and semiconductors. ZnO can absorb a wide range of UV light (λ<400 nm) which could convert photonic energy to excitation energy [2]. Therefore, ZnO could especially be used in shielding UV irradiation, which is beneficial to applications of buildings or automobiles protection. The objective of present work is to improve optical and mechanical properties of PMMA film with ZnO nanoparticles. The effect of concentration of ZnO particles on UV abortion and dynamic mechanical properties was experimentally studied and analyzed.

2. Experimental

In order to prepare composite of PMMA/ZnO, commercial ZnO particles with average size of 20 nm purchased from Wako Pure Chemical Industries and PMMA by Kuraray Co. LTD., were employed.

ZnO nanoparticles with designated loading were mixed with PMMA using a two-roll mill at 200°C for 10 min. The mixed materials were subject to compression molding to prepare 0.5 mm thick sheets. The operating condition of the compression molding machine was 200 °C and 100 MPa. Then the specimen was immersed in 0°C water for cooling down.

The optical properties of prepared specimens were studied by UV–vis-NIR spectrometer (Jasco V570). The scanning speed was 400 nm/min in the wavelength range of 200-800 nm. The nanocomposite film samples were cut into rectangular shapes of 20mm×5mm×0.20mm. Dynamic mechanical analysis of the specimens was performed using a DVE-V4 FT with a heating rate of 1 °C/min and frequency 10 Hz.

3. Results and Discussion

Figure 1(a) shows the absorption spectra of composite with ZnO concentrations of 0.5, 1, 3 and 5 wt%. The intensity of UV absorbance peak increases with ZnO concentration. Although there were some noises in the absorbance curves at a high ZnO concentration, the peak absorption existed at the wavelength of 367 nm, which is smaller than 378 nm (the theoretical wavelength of bulk ZnO corresponding to band-gap of 3.3 eV). The blue-shift phenomenon for 20-nm ZnO particles is attributed to the quantum effect of nanoparticles. Kanemitsu et al.[3] claim that semiconductive nanoparticles would play a role in the electronic interaction due to the

confinement of excitons and electrons in nanoparticles which would lead to efficient energy transfer.
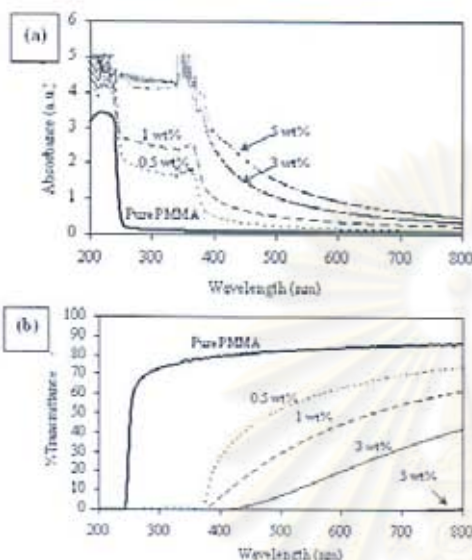
138

Fig. 1 Optical characteristics of PMMA/ZnO nanocomposite films (a) UV absorbance, (b) UV transmittance

Fig.1 (b) shows specific transmission of UV light. It could be clearly observed that only 0.5 wt% of 20-nm ZnO compounded with PMMA could significantly shield UV irradiation, resulting in a remarked decrease in % transmission. Xiong et al. also reported that 7 wt% of 60-nm ZnO particles added into poly(stryrenebutylacrylate) completely shields UV irradiation [4]. As a result, it is reasonable to imply that the nanocomposite prepared in this study would probably exhibit UV protection. Thereby ZnO nanoparticles could improve the UV durability of the PMMA film.

Meanwhile, the loss modulus (E") of the composites was characterized by a dynamic mechanical analyzer (DMA).The loss modulus relates to the energy loss due to polymer chain movement and the E" peak corresponds to the glass transition temperature (T_g). Figure 2 indicates that the T_g of PMMA/ZnO nanocomposites was shifted with the increment of ZnO content and exceeded that of pure PMMA. This would be attributed to the mobility restriction of PMMA chain due to the entangling ZnO particles within PMMA matrix.

4. Conclusions and Recommendations for Thailand

PMMA/ZnO nanocomposite films have been successfully prepared by a two-roll mill. When concentration of ZnO in the composite

was increased, UV absorption of the composite became higher. Based on thermo-mechanical test, the PMMA/ZnO nanocomposite films with higher ZnO content exhibited higher glass transition temperature compared with that of pure PMMA. These results would exhibit possibility to apply PMMA/ZnO composite for UV-cut window, which would be beneficial to many countries including Thailand. However, capability of producing ZnO nanoparticles would be required for Thai manufacturers. Moreover process of manufacturing of UV shielding material should be further studied for finding the most effective route.
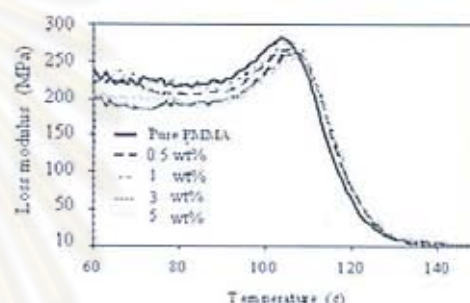

Fig. 2 Effect of ZnO loading on loss modulus of PMMA/ZnO nanocomposite

5. References

[1] P. Yang, H. Yan, S. Mao, R. Russo, J. Johnson, R. Saykally, N. Morris, J. Pham, R. He, H.-J. Choi, Adv. Funct. Mater. 12 (2002) 323–331.

[2] B. Mahltig, H. B. ttcher, K. Rauch, U. Dieckmann, R. Nitsche, T. Fritz, Thin Solid Films 485 (2005) 108–114

[3] Y. Kanemitsu, A. Ishizumi, J. Luminescence 119–120 (2006) 161–166

[4] M. Xiong, G. Gu, B.You, L. Wu, J. Appl. Polym. Sci. 90 (2003) 1923-1931.

Acknowledgement

VITA

Ms. Thornchaya was born June 24, 1984 in Bangkok, Thailand. She started to study in primary and secondary Debsirin Romklao School. In 2005, she received the Bachelor Degree of Engineering (Chemical Engineering) from King Mongkut's Institute of Technology Ladkrabang. Then, she continued to study in Master program in Center of Excellence in Particle Technology (CEPT) at Chemical Engineering Department, Faculty of Engineering, Chulalongkorn University with the master thesis entitled "Gas - Phase Synthesis of Zinc Oxide Nanoparticles for Photoluminescent Polymeric Film Application''